Journal of Nonlinear Modeling and Analysis
Volume 7, Number 4, August 2025, 1274–1306
https://journal.global-sci.org/jnma
DOI:10.12150/jnma.2025.1274

Numerical Analysis of a New COVID-19 Control Model Incorporating Three Different Fractional Operators

William Atokolo[1,†], Remigius Okeke Aja[2], David Omale[1], Godwin Onuche Acheneje[1], Rose Veronica Paul[1] and Jeremiah Amos[1]

Abstract The ongoing COVID-19 pandemic, caused by the highly contagious coronavirus, poses significant challenges to public health worldwide. Effective control measures are essential to mitigate the spread of the virus and protect vulnerable populations. This study aims to develop novel mathematical models using fractional derivatives to analyze the dynamics of the COVID-19 outbreak. By employing modified mathematical procedures, we explore the impact of quarantine and isolation as control measures on the disease's transmission dynamics. We investigate a system representing COVID-19 through three different arbitrary-order derivative operators: the Atangana-Baleanu derivative with the generalized Mittag-Leffler function, the Caputo derivative with a power law, and the Caputo-Fabrizio derivative with exponential decay. Using fixed-point theory, we assess the existence and uniqueness of solutions for the arbitrary-order system. Our analysis includes numerical simulations that reveal how varying the fractional order influences the behavior of the epidemic. The results demonstrate that increasing the fractional order generally slows the disease's progression, reflecting the memory effect inherent in fractional derivatives. Specifically, higher values of the fractional order correspond to a more gradual spread, reducing the peak number of infections and extending the outbreak's duration. The work highlights the critical importance of using fractional order models to capture the complex dynamics of disease spread and emphasizes that the implementation of quarantine and isolation for treatment significantly decreases the cumulative number of new cases and the overall transmission rate of COVID-19. This research underscores the effectiveness of utilizing fractional-order models to better understand and control the complex dynamics of disease transmission.

Keywords Existence and uniqueness, fractional operators, numerical analysis, Adams Bashforth Moulton method, fixed point theory

MSC(2010) 00A71

[†]the corresponding author.
Email address:williamsatokolo@gmail.com(William Atokolo)
[1]Department of Mathematical Sciences, Prince Abubakar Audu University, Anyigba, 272102, Nigeria
[2]Department of Mathematics, Michael Okpara University of Agriculture, Umudike, 440101, Nigeria

1. Introduction

An extension of integer-order derivatives and integrals to arbitrary-order derivatives is known as the calculus of arbitrary-order derivatives. In the field of applied mathematics, fractional calculus has become a potent tool for solving real-world problems. Compared to classical integer-order operators, arbitrary-order operators offer a greater capacity to capture the memory and inheritance aspects of real-world situations.

The applications of arbitrary-order derivatives are extremely varied and include signal processing, biomathematics, engineering, and physics [1, 2], among other domains [3–9]. Numerous arbitrary-order derivatives in fractional calculus (FC) exist and are typically classified into two types in the literature: singular and non-singular.

The most widely used of them are the Riemann-Liouville and Caputo operators [10], which are based on the power law kernel. The idea of arbitrary-order differentiation and integration incorporating a power law kernel has recently undergone historical evolution, where the power law kernel has been examined and modified by a non-singular kernel [11, 12].

In fractional modeling of real-world problems, two widely used derivatives are the Caputo-Fabrizio (CF) derivative, which involves the exponential law kernel [12], and the Atangana-Baleanu (AB) fractional derivative, which was developed based on the Mittag-Leffler kernel with non-local and non-singular properties [11].

Numerous investigators have focused on the scientific applications of these variable-order derivative operators to identify the mathematical systems that these three kinds of kernels are used to describe [13–19].

It can be difficult to pinpoint a specific remedy to an issue at times. Many researchers are naturally more interested in finding fractional operators and using numerical techniques to solve problems as a result of this predicament. The arbitrary-order differential equations can be solved using a variety of numerical methods [20–24].

Researchers have focused more on modeling and analyzing infectious diseases in the bio-mathematical sciences using fractional operators in recent years; some notable studies in this area may be found in [25–32]. Many nations have recently experienced an epidemic of COVID-19, a deadly disease that goes untreated. Since the start of the pandemic, the number of cases of SARS-CoV-2 disease, also known as COVID-19, has been rapidly increasing, making it a serious concern. The recently identified virus from the SARS-CoV-2 virus family is the cause of the respiratory disease COVID-19.

The most typical signs and symptoms of COVID-19 include fever, exhaustion, dry cough, and dyspnea. Human-to-human transmission of the disease is mostly through tiny droplets released during coughing, sneezing, or talking. After being originally discovered in Wuhan, China, in December 2019, the SARS-CoV-2 virus quickly spread to other parts of the world. Numerous people have died as a result of the new outbreak throughout many nations.

Humanity was thrust into a state of extreme fear by the novel COVID-19 outbreak, which compelled people to concentrate their efforts on studying and forecasting the disease's future course. When it comes to understanding how diseases spread, predicting the future, and making decisions to stop the spread of infectious diseases, mathematical systems have been extremely important.

Different mathematical approaches have been developed specifically to explore the COVID-19 pandemic as seen in the works of [33–38]. Also, Khan et al. [39] developed a mathematical model for COVID-19 dynamics using both integer order and Atangana-Baleanu derivative approaches, analyzing stability through fractional Lyapunov functions and implementing numerical solutions via modified Adams-Bashforth scheme. Kumar et al. [40] investigated COVID-19 dynamics using three different fractional derivative approaches (Caputo, Caputo-Fabrizio, and Atangana-Baleanu), analyzing existence and uniqueness through fixed-point theory and providing numerical solutions with varying arbitrary power values. Ghanbari and Kumar [41] studied a fractional predator-prey-pathogen model using Atangana-Baleanu operators, analyzing equilibrium stability, solution uniqueness, and chaotic behaviors through numerical simulations with various fractional derivative values. Kumar et al. [42] analyzed COVID-19 spread in India using Hermite wavelets basis for solving a fractional-order model with Caputo derivative, employing operational matrix with collocation scheme and providing numerical simulations for different fractional orders. Kumar et al. [43] developed a three-dimensional fractional host-parasitoid population model using Caputo operator, investigating chaotic behaviors and providing numerical solutions through Adam-Bashforth-Moulton and Toufik-Atangana schemes. Veeresha et al. [44] investigated fractional generalized nonlinear Schrödinger equation using ν-homotopy analysis transform method with Atangana-Baleanu derivative, proving the existence of solution and demonstrating numerical validations through case studies.

Despite the aforementioned research works on modeling the transmission dynamics of COVID-19, there still exists a significant gap in devising measures to reduce the burden of the disease. Thus, the novelty of this research lies in investigating the effect of fractional order on the transmission dynamics of COVID-19 in the presence of quarantine and isolation for treatment as control measures. In achieving this aim, we examine the COVID-19 mathematical system within the structure of fractional derivative operators using three distinct kernel types with the specific aim of investigating the effect of fractional order, quarantine, and treatment on the transmission dynamics of COVID-19. The advantages of the suggested approach using fractional operators over existing methods are significant. First, fractional order derivatives can approximate real data with greater flexibility than classical derivatives. Second, this approach accounts for non-locality, a feature that classical derivatives cannot capture. Additionally, fractional order derivatives exhibit a memory effect with remarkable characteristics that cannot be replicated in classical models. The memory effect in fractional models can be adjusted to achieve various degrees of responses, providing a more nuanced understanding of the system being studied. Also, the fractional derivative epidemic models provide powerful and hereditary properties of the system, which are neglected or difficult to incorporate in classical models. Futhermore, when fitting data, the fractional models have one more degree of freedom than the integer-order model, which gives several better responses. This can be seen in the work of Chen et al. [45], where they demonstrated that the fractional order model can predict the number of infectious people accurately and help concerned bodies, such as policymakers, stakeholders, and health professionals, make well-informed decisions in preventing and controlling an epidemic.

Using the recommended numerical techniques, the approximate solution is obtained for all the fractional operators that are proposed. A significant limitation of using fractional order models to analyze the spread of infectious diseases is the risk

of over-fitting, as their flexibility can capture noise rather than meaningful patterns. To address this, we implemented cross-validation techniques to evaluate model performance on unseen data, ensuring robust generalization. We also simplified the model by reducing the number of parameters, enhancing its predictive capability as seen in table (1) and table (2). Additionally, we conducted temporal and spatial validation to confirm that the model generalizes effectively across different time periods and geographical contexts. The remaining portion of this work is defined as follows: The mathematical preliminary for the fractional order derivatives is given in Section (1.1). We presented in Section (2), the mathematical model formulation for both classical and fractional orders. Numerical methods for fractional Caputo derivative with power law and that of Caputo-Fabrizio derivative with an exponential law were presented in section (3), with the existence and uniqueness of the model solutions examined alongside the numerical scheme in the same section.

The analysis of the COVID-19 fractional order model via the Atangana-Baleanu (AB) derivative operator and the model simulation are provided in Section (4). In Section (5), conclusion and numerical findings are presented.

1.1. Fractional calculus preliminaries

Some basic definitions and results needed for this study are presented in this section. Important definitions involving the different kernels required for this research are discussed briefly. [46–52].

Definition 1.1. [10]. The Liouville-Caputo fractional order derivative of order $\theta \in [0,1)$ is defined as:

$$ {}_0^C D_t^\theta x(t) = \frac{1}{\Gamma(1-\theta)} \int_0^t (t-\psi)^{-\theta} \frac{d}{dt} x(\psi)\, d\psi. \tag{1.1} $$

Definition 1.2. [12] The Caputo-Fabrizio (CF) derivative that has no singular kernel of a function $x(t)$ of the fractional order $\theta \in (0,1)$ is defined as:

$$ {}_0^{CF} D_t^\theta x(t) = \frac{N(\theta)}{1-\theta} \int_0^t \exp\left[-\frac{\theta(t-\psi)}{1-\theta}\right] \frac{d}{dt} x(\psi)\, d\psi, \tag{1.2} $$

where $N(\theta) = N(0) = N(1)$. Secondly, $x \in Q^{'}(0,T), T > 0$.

Definition 1.3. [53]. For the function $x(t)$, the fractional order integral with order $\theta \in (0,1)$ is defined as:

$$ {}_0^{CF} I_t^\theta x(t) = \frac{2(1-\theta)}{(2-\theta)N(\theta)} x(t) + \frac{2\theta}{(2-\theta)N(\theta)} \int_0^t x(\psi)\, d\psi. \tag{1.3} $$

Definition 1.4. [11]. The Atagana-Baleanu (AB) fractional order operator of order $\theta \in (0,1)$ in Caputo sense is defined as:

$$ {}_0^{ABC} D_t^\theta x(t) = \frac{AB(\theta)}{(1-\theta)} \int_0^t \gamma_0 \left[-\frac{\theta(t-\psi)^\theta}{1-\theta}\right] \frac{d}{dt} x(\psi)\, d\psi, \tag{1.4} $$

where γ_θ is a Mittag-Leffler function and is defined as:

$$\gamma_\theta(m) = \sum_{k=0}^{\infty} \frac{m^k}{\left|(\theta k+1)\right.}, \theta \in C, R(\theta) > 0, m \in C,$$

also $AB(\theta) = 1 - \theta + \frac{\theta}{\left|(\theta)\right.}$ represents the normalization function.

The fractional order integral discussion related to the Atagana-Baleanu derivative is defined as:

$${}_0^{AB}I_t^\theta x(t) = \frac{(1-\theta)}{AB(\theta)} x(t) + \frac{\theta}{AB(\theta)\left|(\theta)\right.} \int_0^t (t-\psi)^{\theta-1} x(\psi)\, d\psi. \tag{1.5}$$

2. Mathematical model formulation

We divide the human population into five compartments, the Susceptible Individuals (S), the Exposed Individuals (E), the Quarantined Individuals (Q), the Infected but Isolated for Treatment Individuals (I_T) and the Recovered Individuals (R).

Susceptible Individuals (S): The population of susceptible individuals is recruited at a constant rate, denoted by Λ, which represents the birth rate and immigration into the population. The class decreases due to natural mortality at a rate μ, reflecting the average lifespan of individuals. Additionally, susceptible individuals can become infected through two main routes: contact with exposed individuals at a transmission rate β_1, and contact with infected individuals who are isolated for treatment at a transmission rate β_2. The parameter β_1 models the rate at which exposed individuals, who are in the incubation phase, transmit the disease to susceptible individuals. On the other hand, β_2 accounts for the possibility that isolated infected individuals may still transmit the virus under certain circumstances, such as ineffective isolation or late detection. The susceptible population also increases when recovered individuals lose their immunity and re-enter the susceptible class at a rate ω, representing the waning immunity observed in some individuals after recovery. Furthermore, individuals who were quarantined but found to be free of COVID-19 after diagnosis may return to the susceptible population at a rate λ, indicating the reintroduction of these individuals into the community after being cleared of the disease. The dynamics of this class is therefore formulated as:

$$\frac{dS}{dt} = \Lambda - \beta_1 SE - \beta_2 SI_T + \lambda Q + \omega R - \mu S.$$

Exposed Individuals (E): The population of exposed individuals increases as a result of new infections, which occur when susceptible individuals come into contact with exposed individuals and infected but isolated individuals at rates β_1 and β_2, respectively. The exposed class decreases at the rate α_1, representing the progression of exposed individuals to fully infected status, at which point they are moved to an isolation center for treatment. Another significant reduction in the exposed population occurs at the rate τ, which corresponds to the quarantine of individuals whose COVID-19 infection status is not yet confirmed. This parameter τ reflects the rate at which individuals exhibiting symptoms or identified as potential cases are temporarily removed from the general population to undergo diagnostic testing.

This process helps to prevent further transmission while awaiting confirmation of the disease. If these quarantined individuals are diagnosed as negative, they may return to the susceptible class; otherwise, they progress into the appropriate infection categories. Finally, the exposed class also decreases due to natural mortality at the rate μ. The overall dynamics of the exposed population are thus formulated as:

$$\frac{dE}{dt} = \beta_1 SE + \beta_2 SI_T - \alpha_1 E - \tau E - \mu E.$$

Quarantined Individuals (Q): The population of quarantined individuals increases at the rate τ, which represents the transfer of unconfirmed COVID-19 cases from the exposed class into quarantine for diagnostic testing. This quarantined class decreases as individuals who are diagnosed to be free of COVID-19 return to the susceptible population at a rate λ. The parameter λ captures the reintegration of these individuals into the community after testing negative, thereby reducing the number of quarantined individuals. Additionally, the quarantined class decreases at the rate α_2, which accounts for the progression of those diagnosed as COVID-19 positive. These individuals are transferred to an isolation center for medical treatment to prevent further transmission and to receive care. Finally, similar to other classes, the quarantined population is subject to natural mortality at the rate μ. The overall dynamics of the quarantined population are thus formulated as:

$$\frac{dQ}{dt} = \tau E - \lambda Q - \alpha_2 Q - \mu Q.$$

Infected but Isolated for Treatment Individuals (I_T): The population of infected individuals who are isolated for treatment increases through two main processes. First, exposed individuals who become fully infectious are transferred to this class at a rate α_1, representing the progression from the exposed stage to active infection requiring isolation. Second, quarantined individuals who are confirmed to be COVID-19 positive after diagnostic testing are moved to the isolation center for treatment at a rate α_2. These transfers help in segregating infectious individuals from the general population to reduce transmission risks. The size of the isolated infected population decreases due to recovery after treatment, which occurs at a rate ϕ. The parameter ϕ reflects the effectiveness of medical treatment in reducing the number of active cases. Additionally, this class reduces due to deaths caused by the disease at a rate σ, representing disease-induced mortality, and from natural deaths at a rate μ. Together, these factors shape the overall dynamics of the isolated infected population, which are formulated as:

$$\frac{dI_T}{dt} = \alpha_1 E + \alpha_2 Q - \phi I_T - \sigma I_T - \mu I_T.$$

Recovered Individuals (R): The population of recovered individuals increases at a rate ϕ, which corresponds to the recovery of infected individuals following treatment. This recovery signifies the transition from the isolated infected class back to the recovered class, reflecting the effectiveness of medical interventions in curing COVID-19. However, the recovered population also experiences a decrease as individuals lose their immunity and become susceptible to reinfection at a rate ω. This parameter ω captures the phenomenon of waning immunity, where individuals who have recovered from COVID-19 may not maintain long-term protection against

the virus. Finally, the recovered class decreases due to natural mortality at a rate μ, which affects all individuals in the population regardless of their infection status. The dynamics of the recovered population are thus formulated as:

$$\frac{dR}{dt} = \phi I_T - \omega R - \mu R.$$

The flow diagram that is associated with the above description is shown in Fig. (1)

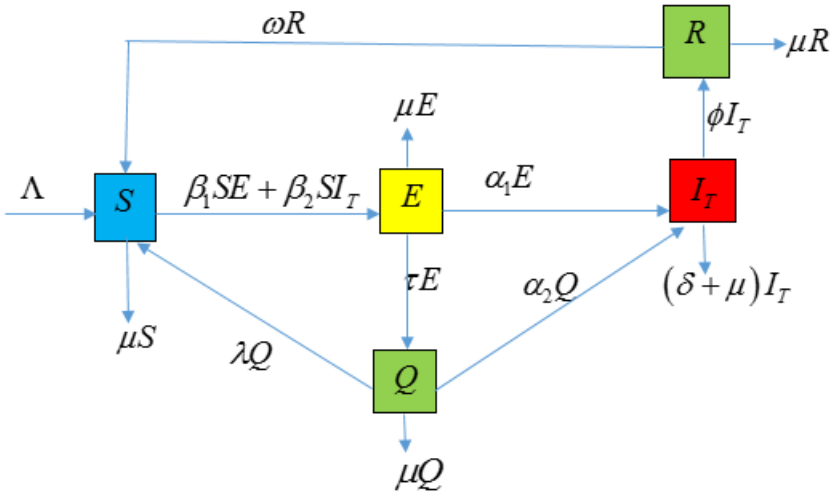

Figure 1. Flow diagram for the COVID-19 model

The mathematical model associated with our assumptions and the above model description is given by

$$\left.\begin{aligned}
\tfrac{dS}{dt} &= \Lambda - \beta_1 SE - \beta_2 SI_T + \lambda Q + \omega R - \mu S,\\
\tfrac{dE}{dt} &= \beta_1 SE + \beta_2 SI_T - \alpha_1 E - \tau E - \mu E,\\
\tfrac{dQ}{dt} &= \tau E - \lambda Q - \alpha_2 Q - \mu Q,\\
\tfrac{dI_T}{dt} &= \alpha_1 E + \alpha_2 Q - \phi I_T - \sigma I_T - \mu I_T,\\
\tfrac{dR}{dt} &= \phi I_T - \omega R - \mu R.
\end{aligned}\right\} \tag{2.1}$$

2.1. Fractional COVID-19 mathematical model

We extend in this section the integer model presented in equation (2.1) as follows:

$$\left.\begin{aligned}
D_t S(t) &= \Lambda - \beta_1 SE - \beta_2 SI_T + \lambda Q + \omega R - \mu S,\\
D_t E(t) &= \beta_1 SE + \beta_2 SI_T - \alpha_1 E - \tau E - \mu E,\\
D_t Q(t) &= \tau E - \lambda Q - \alpha_2 Q - \mu Q,\\
D_t I_T(t) &= \alpha_1 E + \alpha_2 Q - \phi I_T - \sigma I_T - \mu I_T,\\
D_t R(t) &= \phi I_T - \omega R - \mu R,
\end{aligned}\right\} \tag{2.2}$$

with initial conditions

$$S_0(t) = S(0),\ E_0(t) = E(0),\ Q_0(t) = Q(0),\ I_{T0}(t) = I_T(0),\ R_0(t) = R(0).$$

Model (2.2) is therefore re-modeled by replacing the classical derivative (D_t) using $\left({}_0^C D_t^\theta\right)$, $\left({}_0^{CF} D_t^\theta\right)$ and $\left({}_0^{ABC} D_t^\theta\right)$ which represents the Caputo derivative with fractional order θ, Caputo-Fabrizio derivative with fractional order θ and Atagana-Baleanu derivative with fractional order θ respectively.

The modified COVID-19 model with Caputo derivative of fractional order θ with power law is presented as:

$$\left.\begin{aligned}
{}_0^C D_t^\theta S(t) &= \Lambda - \beta_1 SE - \beta_2 SI_T + \lambda Q + \omega R - \mu S,\\
{}_0^C D_t^\theta E(t) &= \beta_1 SE + \beta_2 SI_T - \alpha_1 E - \tau E - \mu E,\\
{}_0^C D_t^\theta Q(t) &= \tau E - \lambda Q - \alpha_2 Q - \mu Q,\\
{}_0^C D_t^\theta I_T(t) &= \alpha_1 E + \alpha_2 Q - \phi I_T - \sigma I_T - \mu I_T,\\
{}_0^C D_t^\theta R(t) &= \phi I_T - \omega R - \mu R.
\end{aligned}\right\} \tag{2.3}$$

The modified COVID-19 model with Caputo-Fabrizio derivative of fractional order θ, which has an exponential kernel law is presented as:

$$\left.\begin{aligned}
{}_0^{CF} D_t^\theta S(t) &= \Lambda - \beta_1 SE - \beta_2 SI_T + \lambda Q + \omega R - \mu S,\\
{}_0^{CF} D_t^\theta E(t) &= \beta_1 SE + \beta_2 SI_T - \alpha_1 E - \tau E - \mu E,\\
{}_0^{CF} D_t^\theta Q(t) &= \tau E - \lambda Q - \alpha_2 Q - \mu Q,\\
{}_0^{CF} D_t^\theta I_T(t) &= \alpha_1 E + \alpha_2 Q - \phi I_T - \sigma I_T - \mu I_T,\\
{}_0^{CF} D_t^\theta R(t) &= \phi I_T - \omega R - \mu R.
\end{aligned}\right\} \tag{2.4}$$

Also the modified COVID-19 model with Atagana-Baleanu-derivative with generalized Mittag-Leffler function is presented as:

$$\left.\begin{aligned}
{}_0^{ABC} D_t^\theta S(t) &= \Lambda - \beta_1 SE - \beta_2 SI_T + \lambda Q + \omega R - \mu S,\\
{}_0^{ABC} D_t^\theta E(t) &= \beta_1 SE + \beta_2 SI_T - \alpha_1 E - \tau E - \mu E,\\
{}_0^{ABC} D_t^\theta Q(t) &= \tau E - \lambda Q - \alpha_2 Q - \mu Q,\\
{}_0^{ABC} D_t^\theta I_T(t) &= \alpha_1 E + \alpha_2 Q - \phi I_T - \sigma I_T - \mu I_T,\\
{}_0^{ABC} D_t^\theta R(t) &= \phi I_T - \omega R - \mu R.
\end{aligned}\right\} \tag{2.5}$$

3. Numerical method for the Caputo derivative

We introduce briefly the predictor-Corrector type numerical algorithm to solve COVID-19 model with Caputo derivative of fractional order (θ).

$$\left.\begin{aligned}
{}_0^C D_t^\theta x(t) &= F(t, x(t)), 0 \le t \le T,\\
x^{(n)}(0) &= x_0^{(n)}, n = 0, 1, 2, ...k-1.
\end{aligned}\right\} \tag{3.1}$$

Equation (3.1) is the same as the Volterra integral equation.

$$x(t) = \sum_{n=0}^{|\theta|-1} x_0^{(n)} \frac{t^n}{n!} + \frac{1}{\overline{|(\theta)}} \int_0^t \frac{F(\psi, x(\psi))}{(t-\psi)^{1-\theta}} d\psi. \tag{3.2}$$

Setting $P = \frac{T}{N}$, $t_r = rp, (r = 0, 1, 2, 3, ...R)$.

We therefore discretize equation (3.2) as follows:

$$x_p(t_{r+1}) = \sum_{n=0}^{|\theta|-1} \frac{t_{r+1}^n}{n!} x_0^{(n)} + \frac{P^\theta}{\overline{|(\theta+2)}} \left[F\left(t_{r+1}, x_P^V(t_{r+1})\right) + \sum_{i=0}^{k} b_{i,k+1} F(t_i, x_r(t_i)) \right], \tag{3.3}$$

where $x_p(t_{r+1})$ is called the predicted value which is evaluated using the arbitrary Adams-Bashforth method as given below:

$$x_P^V(t_{r+1}) = \sum_{n=0}^{|\theta|-1} \frac{t_{r+1}^n}{n!} x_0^{(n)} + \frac{1}{\overline{|(\theta)}} \sum_{i=0}^{k} d_{i,k+1} F(t_i, x_r(t_i)), \tag{3.4}$$

where

$$b_{i,k+1} = \begin{cases} r^{\theta+1} - (r-\theta)(r+1)^\theta, i = 0, \\ (r-i+2)^{\theta+1} + (r-i)^{\theta+1} - 2(r-i+1)^{\theta+1}, 1 \le i \le r, \\ 1. i = r+1, \end{cases}$$

and

$$d_{i,k+1} = \frac{P^\theta}{\theta} \left((r+1-i)^\theta - (r-i)^\theta \right), 0 \le i \le k, i = 1, 2, 3.$$

3.1. Predictor-corrector numerical method for the COVID-19 model with Caputo fractional derivative

From our model (2.3), we employ the predictor-corrector numerical method to solve the fractional operator. Model (2.3) to this end is discretized as follows:

$$\begin{aligned}
S_{r+1} &= S(0) + \frac{P^\theta}{|\overline{\theta+2}|} \left[F_1\left(t_{r+1}, S_{r+1}^V, E_{r+1}^V, Q_{r+1}^V, I_{Tr+1}^V, R_{r+1}^V\right) + \sum_{i=0}^{k} b_{i,k+1} F_1\left(t_i, S_i, E_i, Q_i, I_{Ti}, R_i\right) \right], \\
E_{r+1} &= E(0) + \frac{P^\theta}{|\overline{\theta+2}|} \left[F_2\left(t_{r+1}, S_{r+1}^V, E_{r+1}^V, Q_{r+1}^V, I_{Tr+1}^V, R_{r+1}^V\right) + \sum_{i=0}^{k} b_{i,k+1} F_2\left(t_i, S_i, E_i, Q_i, I_{Ti}, R_i\right) \right], \\
Q_{r+1} &= Q(0) + \frac{P^\theta}{|\overline{\theta+2}|} \left[F_3\left(t_{r+1}, S_{r+1}^V, E_{r+1}^V, Q_{r+1}^V, I_{Tr+1}^V, R_{r+1}^V\right) + \sum_{i=0}^{k} b_{i,k+1} F_3\left(t_i, S_i, E_i, Q_i, I_{Ti}, R_i\right) \right], \\
I_{Tr+1} &= I_T(0) + \frac{P^\theta}{|\overline{\theta+2}|} \left[F_4\left(t_{r+1}, S_{r+1}^V, E_{r+1}^V, Q_{r+1}^V, I_{Tr+1}^V, R_{r+1}^V\right) + \sum_{i=0}^{k} b_{i,k+1} F_4\left(t_i, S_i, E_i, Q_i, I_{Ti}, R_i\right) \right], \\
R_{r+1} &= R(0) + \frac{P^\theta}{|\overline{\theta+2}|} \left[F_5\left(t_{r+1}, S_{r+1}^V, E_{r+1}^V, Q_{r+1}^V, I_{Tr+1}^V, R_{r+1}^V\right) + \sum_{i=0}^{k} b_{i,k+1} F_5\left(t_i, S_i, E_i, Q_i, I_{Ti}, R_i\right) \right].
\end{aligned} \tag{3.5}$$

$S_{r+1}^V, E_{r+1}^V, Q_{r+1}^V, T_{Tr+1}^V, R_{r+1}^V$ are therefore written as follows:

$$\left.\begin{aligned}
S_{r+1}^{V} &= S(0) + \tfrac{1}{|(\theta)} \left[\sum_{i=0}^{k} d_{i,k+1} F_1(t_i, S_i, E_i, Q_i, I_{Ti}, R_i)\right], \\
E_{r+1}^{V} &= E(0) + \tfrac{1}{|(\theta)} \left[\sum_{i=0}^{k} d_{i,k+1} F_2(t_i, S_i, E_i, Q_i, I_{Ti}, R_i)\right], \\
Q_{r+1}^{V} &= Q(0) + \tfrac{1}{|(\theta)} \left[\sum_{i=0}^{k} d_{i,k+1} F_3(t_i, S_i, E_i, Q_i, I_{Ti}, R_i)\right], \\
I_{Tr+1}^{V} &= I_T(0) + \tfrac{1}{|(\theta)} \left[\sum_{i=0}^{k} d_{i,k+1} F_4(t_i, S_i, E_i, Q_i, I_{Ti}, R_i)\right], \\
R_{r+1}^{V} &= R(0) + \tfrac{1}{|(\theta)} \left[\sum_{i=0}^{k} d_{i,k+1} F_5(t_i, S_i, E_i, Q_i, I_{Ti}, R_i)\right],
\end{aligned}\right\} \tag{3.6}$$

where

$$\left.\begin{aligned}
F_1(t, S, E, Q, I_T, R) &= \Lambda - \beta_1 SE - \beta_2 SI_T + \lambda Q + \omega R - \mu S, \\
F_2(t, S, E, Q, I_T, R) &= \beta_1 SE + \beta_2 SI_T - \alpha_1 E - \tau E - \mu E, \\
F_3(t, S, E, Q, I_T, R) &= \tau E - \lambda Q - \alpha_2 Q - \mu Q, \\
F_4(t, S, E, Q, I_T, R) &= \alpha_1 E + \alpha_2 Q - \phi I_T - \sigma I_T - \mu I_T, \\
F_5(t, S, E, Q, I_T, R) &= \phi I_T - \omega R - \mu R.
\end{aligned}\right\} \tag{3.7}$$

3.2. Existence and uniqueness of solutions for the modified COVID-19 model with Caputo-Fabrizio derivative

In this section, we employ the fixed point theorem to investigate the existence and uniqueness of solution for the modified COVID-19 model with Caputo-Fabrizio derivative presented in equation (2.4).

The model is therefore transformed into an integral equation given as:

$$\left.\begin{aligned}
S(t) - S(0) &= {}_0^{CF} I_t^{\theta} \left[\Lambda - \beta_1 SE - \beta_2 SI_T + \lambda Q + \omega R - \mu S\right], \\
E(t) - E(0) &= {}_0^{CF} I_t^{\theta} \left[\beta_1 SE + \beta_2 SI_T - \alpha_1 E - \tau E - \mu E\right], \\
Q(t) - Q(0) &= {}_0^{CF} I_t^{\theta} \left[\tau E - \lambda Q - \alpha_2 Q - \mu Q\right], \\
I_T(t) - I_T(0) &= {}_0^{CF} I_t^{\theta} \left[\alpha_1 E + \alpha_2 Q - \phi I_T - \sigma I_T - \mu I_T\right], \\
R(t) - R(0) &= {}_0^{CF} I_t^{\theta} \left[\phi I_T - \omega R - \mu R\right].
\end{aligned}\right\} \tag{3.8}$$

The kernel is defined as follows:

$$\left.\begin{aligned}
Y_1(t, S) &= \Lambda - \beta_1 SE - \beta_2 SI_T + \lambda Q + \omega R - \mu S, \\
Y_2(t, E) &= \beta_1 SE + \beta_2 SI_T - \alpha_1 E - \tau E - \mu E, \\
Y_3(t, Q) &= \tau E - \lambda Q - \alpha_2 Q - \mu Q, \\
Y_4(t, I_T) &= \alpha_1 E + \alpha_2 Q - \phi I_T - \sigma I_T - \mu I_T, \\
Y_5(t, R) &= \phi I_T - \omega R - \mu R.
\end{aligned}\right\} \tag{3.9}$$

We obtain the following after using the arbitrary integral in equation (3.8).

$$\left.\begin{aligned}
S(t)-S(0)&=\tfrac{2(i-\theta)}{(2-\theta)N(\theta)}Y_1(t,S)+\tfrac{2\theta}{(2-\theta)N(\theta)}\int_0^t Y_1(\phi,S)\,d\phi,\\
E(t)-E(0)&=\tfrac{2(i-\theta)}{(2-\theta)N(\theta)}Y_2(t,S)+\tfrac{2\theta}{(2-\theta)N(\theta)}\int_0^t Y_2(\phi,S)\,d\phi,\\
Q(t)-Q(0)&=\tfrac{2(i-\theta)}{(2-\theta)N(\theta)}Y_3(t,S)+\tfrac{2\theta}{(2-\theta)N(\theta)}\int_0^t Y_3(\phi,S)\,d\phi,\\
I_T(t)-I_T(0)&=\tfrac{2(i-\theta)}{(2-\theta)N(\theta)}Y_4(t,S)+\tfrac{2\theta}{(2-\theta)N(\theta)}\int_0^t Y_4(\phi,S)\,d\phi,\\
R(t)-R(0)&=\tfrac{2(i-\theta)}{(2-\theta)N(\theta)}Y_5(t,S)+\tfrac{2\theta}{(2-\theta)N(\theta)}\int_0^t Y_5(\phi,S)\,d\phi.
\end{aligned}\right\}\tag{3.10}$$

Theorem 3.1. *The kernels Y_1, Y_2, Y_3, Y_4 and Y_5 in equation (3.9) fulfill the Lipschitz and contraction condition provided that the inequality given below is satisfied*

$$0 \leq (\beta_1 g_2 + \beta_2 g_4 + \mu g_1) < 1.$$

Proof. Starting with kernel Y_1 and assuming that kernel Y_1, has S and S^* as functions, then we can say

$$\begin{aligned}
&\|Y_1(t,S)-Y_1(t,S^*)\|\\
&=\|-(\beta_1 E+\beta_2 I_T+\mu)S-S^*\|\\
&\leq(\beta_1\|E\|+\beta_2\|I_T\|+\mu)\|S-S^*\|\\
&\leq(\beta_1 g_2+\beta_2 g_4+\mu g_1)\|S-S^*\|.
\end{aligned}\tag{3.11}$$

Let $L_1 = (\beta_1 g_2 + \beta_2 g_4 + \mu g_1)$. Considering the fact that

$$\|S\| \leq g_1, \|E\| \leq g_2, \|Q\| \leq g_3, \|I_T\| \leq g_4, \|R\| \leq g_5$$

are functions that are bounded where g_1, g_2, g_3, g_4 and g_5 are some non-negative constants. We therefore have that:

$$\|Y_1(t,S)-Y_1(t,S^*)\| \leq \rho_1\|S-S^*\|. \tag{3.12}$$

Equation (3.12) means kernel Y_1 satisfies the Lipschitz condition. For the contraction condition, $0 \leq \rho_1 < 1$ settles the case.

Similarly, we can write expressions for the remaining kernels as follows:

$$\left.\begin{aligned}
\|Y_2(t,E)-Y_2(t,E^*)\| &\leq \rho_2\|E-E^*\|,\\
\|Y_3(t,E)-Y_3(t,E^*)\| &\leq \rho_3\|Q-Q^*\|,\\
\|Y_4(t,E)-Y_4(t,E^*)\| &\leq \rho_4\|I_T-{I_T}^*\|,\\
\|Y_5(t,E)-Y_5(t,E^*)\| &\leq \rho_5\|R-R^*\|.
\end{aligned}\right\}\tag{3.13}$$

Introducing the recursive formula using equation (3.10) gives:

$$\left.\begin{aligned}
S_r(t) &= \tfrac{2(1-\theta)}{(2-\theta)N(\theta)} Y_1(t, S_{r-1}) + \tfrac{2\theta}{(2-\theta)N(\theta)} \int_0^t Y_1(\phi, S_{r-1})\, d\phi, \\
E_r(t) &= \tfrac{2(1-\theta)}{(2-\theta)N(\theta)} Y_2(t, E_{r-1}) + \tfrac{2\theta}{(2-\theta)N(\theta)} \int_0^t Y_2(\phi, E_{r-1})\, d\phi, \\
Q_r(t) &= \tfrac{2(1-\theta)}{(2-\theta)N(\theta)} Y_3(t, Q_{r-1}) + \tfrac{2\theta}{(2-\theta)N(\theta)} \int_0^t Y_3(\phi, Q_{r-1})\, d\phi, \\
I_{Tr}(t) &= \tfrac{2(1-\theta)}{(2-\theta)N(\theta)} Y_4(t, I_{Tr-1}) + \tfrac{2\theta}{(2-\theta)N(\theta)} \int_0^t Y_4(\phi, I_{Tr-1})\, d\phi, \\
R_r(t) &= \tfrac{2(1-\theta)}{(2-\theta)N(\theta)} Y_5(t, R_{r-1}) + \tfrac{2\theta}{(2-\theta)N(\theta)} \int_0^t Y_5(\phi, S_{r-1})\, d\phi,
\end{aligned}\right\} \tag{3.14}$$

where $S_0 = S(0), E_0 = E(0), Q_0 = Q(0), I_{T0} = I(T0), R_0 = R(0)$ are the initial conditions for the recursive expression given in (3.14).

Equation (3.15) is obtained after taking the difference between successive terms.

$$\begin{aligned}
\psi_r(t) &= S_r(t) - S_{r-1}(t) = \frac{2(1-\theta)}{(2-\theta)N(\theta)} Y_1(t, S_{r-1}) + \frac{2\theta}{(2-\theta)N(\theta)} \int_0^t Y_1(\phi, S_{r-1}) d\phi, \\
\chi_r(t) &= E_r(t) - E_{r-1}(t) = \frac{2(1-\theta)}{(2-\theta)N(\theta)} Y_2(t, E_{r-1}) + \frac{2\theta}{(2-\theta)N(\theta)} \int_0^t Y_2(\phi, E_{r-1}) d\phi, \\
\pi_r(t) &= Q_r(t) - Q_{r-1}(t) = \frac{2(1-\theta)}{(2-\theta)N(\theta)} Y_3(t, Q_{r-1}) + \frac{2\theta}{(2-\theta)N(\theta)} \int_0^t Y_3(\phi, Q_{r-1}) d\phi, \\
\Omega_r(t) &= I_{Tr}(t) - I_{Tr-1}(t) = \frac{2(1-\theta)}{(2-\theta)N(\theta)} Y_4(t, I_{T_{r-1}}) + \frac{2\theta}{(2-\theta)N(\theta)} \int_0^t Y_4(\phi, I_{T_{r-1}}) d\phi, \\
\sigma_r(t) &= R_r(t) - R_{r-1}(t) = \frac{2(1-\theta)}{(2-\theta)N(\theta)} Y_5(t, R_{r-1}) + \frac{2\theta}{(2-\theta)N(\theta)} \int_0^t Y_5(\phi, R_{r-1}) d\phi.
\end{aligned} \tag{3.15}$$

Expressing our model variables in terms of an infinite series, we have that

$$\begin{aligned}
&S_r(t) = \sum_{i=1}^{r} \psi_i(t), E_r(t) = \sum_{i=1}^{r} \chi_i(t), Q_r(t) = \sum_{i=1}^{r} \pi_i(t), \\
&I_{Tr}(t) = \sum_{i=1}^{r} \Omega_i(t), R_r(t) = \sum_{i=1}^{r} \sigma_i(t).
\end{aligned}$$

We obtain equation (3.16) by taking the norm of equation (3.15).

$$\|\psi_r(t)\| = \|S_r(t) - S_{r-1}(t)\| = \left\| \tfrac{2(1-\theta)}{(2-\theta)N(\theta)} Y_1(t, S_{r-1}) + \tfrac{2\theta}{(2-\theta)N(\theta)} \int_0^t Y_1(\phi, S_{r-1}) d\phi \right\|. \tag{3.16}$$

Equation(3.16) is modified as (3.17), when we apply the triangle inequality

$$\|\psi_r(t)\| = \|S_r(t) - S_{r-1}(t)\| \leq \tfrac{2(1-\theta)}{(2-\theta)N(\theta)} \|Y_1(t, S_{r-1})\| + \tfrac{2\theta}{(2-\theta)N(\theta)} \left\| \int_0^t Y_1(\phi, S_{r-1}) d\phi \right\|. \tag{3.17}$$

Using the Lipschitz condition which is satisfied from theorem (3.1), Section (3.2) by kernels, we now rewrite equation (3.17) as:

$$\|\psi_r(t)\| = \|S_r(t) - S_{r-1}(t)\| \leq \tfrac{2(1-\theta)}{(2-\theta)N(\theta)} \rho_1 \|S_{r-1} - S_{r-2}\| + \tfrac{2\theta}{(2-\theta)N(\theta)} \rho_1 \int_0^t \|S_{r-1} - S_{r-2}\| d\phi. \tag{3.18}$$

Therefore we have

$$\|\psi_r(t)\| = \|S_r(t) - S_{r-1}(t)\| \leq \frac{2(1-\theta)}{(2-\theta)N(\theta)}\rho_1 \|\psi_{r-1}(t)\| + \frac{2\theta}{(2-\theta)N(\theta)}\rho_1 \int_0^t \|\psi_{r-1}(\phi)\| \, d\phi. \tag{3.19}$$

The following results are obtained following the same procedure used in equation (3.19)

$$\begin{aligned}
\|\chi_r(t)\| &= \|S_r(t) - S_{r-1}(t)\| \leq \frac{2(1-\theta)}{(2-\theta)N(\theta)}\rho_1 \|\chi_{r-1}(t)\| + \frac{2\theta}{(2-\theta)N(\theta)}\rho_1 \int_0^t \|\chi_{r-1}(\phi)\| \, d\phi, \\
\|\pi_r(t)\| &= \|S_r(t) - S_{r-1}(t)\| \leq \frac{2(1-\theta)}{(2-\theta)N(\theta)}\rho_1 \|\pi_{r-1}(t)\| + \frac{2\theta}{(2-\theta)N(\theta)}\rho_1 \int_0^t \|\pi_{r-1}(\phi)\| \, d\phi, \\
\|\Omega_r(t)\| &= \|S_r(t) - S_{r-1}(t)\| \leq \frac{2(1-\theta)}{(2-\theta)N(\theta)}\rho_1 \|\Omega_{r-1}(t)\| + \frac{2\theta}{(2-\theta)N(\theta)}\rho_1 \int_0^t \|\Omega_{r-1}(\phi)\| \, d\phi, \\
\|\sigma_r(t)\| &= \|S_r(t) - S_{r-1}(t)\| \leq \frac{2(1-\theta)}{(2-\theta)N(\theta)}\rho_5 \|\psi_{r-1}(t)\| + \frac{2\theta}{(2-\theta)N(\theta)}\rho_5 \int_0^t \|\sigma_{r-1}(\phi)\| \, d\phi.
\end{aligned} \tag{3.20}$$

□

Theorem 3.2. *The fractional order model (2.4) coupled solution exists, if there exist some t_0 whenever*

$$\frac{2\,(1-\theta)}{(2-\theta)\,N\,(\theta)}\rho_1 + \frac{2\theta}{(2-\theta)}\rho_1 t_0 < 1.$$

Proof. The model variables $S\,(t)\,, E\,(t)\,, Q\,(t)\,, I\,(Tt)$ and $R\,(t)$ are taken to be bounded functions of which Lipschitz condition is fulfilled by their kernels.

We therefore obtain the following results by employing equations (3.19) and (3.20) recursively.

$$\begin{aligned}
\|\psi_r\,(t)\| &\leq \|S\,(0)\| \left[\tfrac{2(1-\theta)}{(2-\theta)N(\theta)}\rho_1 + \tfrac{2(1-\theta)}{(2-\theta)N(\theta)}\rho_1 t\right]^r, \\
\|\chi_r\,(t)\| &\leq \|E\,(0)\| \left[\tfrac{2(1-\theta)}{(2-\theta)N(\theta)}\rho_2 + \tfrac{2(1-\theta)}{(2-\theta)N(\theta)}\rho_2 t\right]^r, \\
\|\pi_r\,(t)\| &\leq \|Q\,(0)\| \left[\tfrac{2(1-\theta)}{(2-\theta)N(\theta)}\rho_3 + \tfrac{2(1-\theta)}{(2-\theta)N(\theta)}\rho_3 t\right]^r, \\
\|\Omega_r\,(t)\| &\leq \|I_T\,(0)\| \left[\tfrac{2(1-\theta)}{(2-\theta)N(\theta)}\rho_4 + \tfrac{2(1-\theta)}{(2-\theta)N(\theta)}\rho_4 t\right]^r, \\
\|\sigma_r\,(t)\| &\leq \|R\,(0)\| \left[\tfrac{2(1-\theta)}{(2-\theta)N(\theta)}\rho_5 + \tfrac{2(1-\theta)}{(2-\theta)N(\theta)}\rho_5 t\right]^r.
\end{aligned} \tag{3.21}$$

We assume the following so as to show that equation (3.21) is a unique solution of the Caputo-Fabrizio derivative COVID-19 model presented in equation (2.4).

$$\left.\begin{aligned}
S\,(t) - S\,(0) &= S_r\,(t) - A_r\,(t)\,, \\
E\,(t) - E\,(0) &= E_r\,(t) - B_r\,(t)\,, \\
Q\,(t) - Q\,(0) &= Q_r\,(t) - C_r\,(t)\,, \\
I_T\,(t) - I_T\,(0) &= I_{Tr}\,(t) - D_r\,(t)\,, \\
R\,(t) - R\,(0) &= R_r\,(t) - F_r\,(t)\,,
\end{aligned}\right\} \tag{3.22}$$

such that

$$\|A_r(t)\| = \left\| \frac{2(1-\theta)}{(2-\theta)N(\theta)} \left(Y_1(t,S) - Y_1(t,S_{r-1})\right) + \frac{2\theta}{(2-\theta)N(\theta)} \int_0^t \left(Y_1(\phi,S) - Y_1(\phi,S_{r-1})\right) d\phi \right\|.$$

$$\leq \frac{2(1-\theta)}{(2-\theta)N(\theta)} \|Y_1(t,S) - Y_1(t,S_{r-1})\| + \frac{2\theta}{(2-\theta)N(\theta)} \int_0^t \|Y_1(\phi,S) - Y_1(\phi,S_{r-1})\| \, d\phi,$$

$$\|A_r(t)\| \leq \frac{2(1-\theta)}{(2-\theta)N(\theta)} \rho_1 \|S - S_{r-1}\| + \frac{2\theta}{(2-\theta)N(\theta)} \|S - S_{r-1}\| t. \tag{3.23}$$

Then,

$$\|A_r(t)\| \leq \left[\frac{2(1-\theta)}{(2-\theta)N(\theta)} \rho_1 + \frac{2\theta}{(2-\theta)N(\theta)} \rho_1 t \right]^{r+1} E. \tag{3.24}$$

When $t = t_0$, we have that

$$\|A_r(t)\| \leq \left[\frac{2(1-\theta)}{(2-\theta)N(\theta)} \rho_1 + \frac{2\theta}{(2-\theta)N(\theta)} \rho_1 t_0 \right]^{r+1} E. \tag{3.25}$$

Taking the limit of equation (3.25) as $r \to \inf$, then we have $\|A_r(t)\|^r$ leading to zero.

In the same way, we can show that $\|B_r(t)\| \to 0$, $\|C_r(t)\| \to 0$, $\|D_r(t)\| \to 0$, $\|F_r(t)\| \to 0$.

We therefore conclude that the existence of the solution to our model (2.4) is proved.

We now discuss the uniqueness of the solution to model (2.4) in Theorem (3.3). □

Theorem 3.3. *The fractional COVID-19 model (2.4) with Caputo-Fabrizio derivative has a unique solution whenever*

$$\left(1 - \frac{2(1-\theta)}{(2-\theta)N(\theta)} \rho_1 - \frac{2\theta}{(2-\theta)N(\theta)} \rho_1 t\right) > 0.$$

Proof. Assuming that the fractional model (2.4) has another solution of the form $S^*(t), E^*(t), Q^*(t), I_T^*(t)$ and $R^*(t)$, therefore

$$S(t) - S^*(t) = \frac{2(1-\theta)}{(2-\theta)N(\theta)} \left(Y_1(t,S) - Y_1(t,S^*)\right) + \frac{2\theta}{(2-\theta)N(\theta)} \int_0^t \left(Y_1(\phi,S) - Y_1(\phi,S^*)\right) d\phi. \tag{3.26}$$

Taking the norm of the above equation (3.26), we have

$$\|S(t) - S^*(t)\| \leq \frac{2(1-\theta)}{(2-\theta)N(\theta)} \|Y_1(t,S) - Y_1(t,S^*)\| + \frac{2\theta}{(2-\theta)N(\theta)} \int_0^t \|Y_1(\phi,S) - Y_1(\phi,S^*)\| \, d\phi. \tag{3.27}$$

Since the Lipschitz condition is satisfied by the kernel, then we have that,

$$\|S(t) - S^*(t)\| \leq \frac{2(1-\theta)}{(2-\theta)N(\theta)} \rho_1 \|S(t) - S^*(t)\| + \frac{2\theta}{(2-\theta)N(\theta)} \rho_1 t \|S(t) - S^*(t)\|. \tag{3.28}$$

Equation (3.28) can also be expressed as

$$\|S(t) - S^*(t)\| \left(1 - \frac{2(1-\theta)}{(2-\theta)N(\theta)}\rho_1 - \frac{\theta}{(2-\theta)N(\theta)}\rho_1 t\right) \leq 0. \tag{3.29}$$

But

$$\|S(t) - S^*(t)\| = 0. \tag{3.30}$$

Therefore

$$S(t) = S^*(t). \tag{3.31}$$

This implies the model solution is proved to be unique. The remaining fractions $E(t), Q(t), I_T(t)$ and $R(t)$ results can be obtained following the same procedure. □

3.3. Caputo-Fabrizio derivative numerical algorithm

In this section, we discussed a numerical method for Caputo-Fabrizio fractional order derivative following the method used in [23].

$${}_0^{CF}D_t^{\theta} x(t) = y(t, x(t)). \tag{3.32}$$

Using the calculus fundamental theorem we now have,

$$x(t) - x(0) = \frac{1-\theta}{N(\theta)} y(t, x(t)) + \frac{\theta}{N(\theta)} \int_0^t y(\psi, x(\psi)) d\psi. \tag{3.33}$$

For a general case (3.33) becomes

$$x(t_{r+1}) - x(0) = \frac{1-\theta}{N(\theta)} y(t_{r+1}, x(t_{r+1})) + \frac{\theta}{N(\theta)} \int_0^{t_{r+1}} y(t, x(t)) dt. \tag{3.34}$$

Secondly,

$$x(t_r) - x(0) = \frac{1-\theta}{N(\theta)} y(t_{r-1}, x(t_{r-1})) + \frac{\theta}{N(\theta)} \int_0^{t_r} y(t, x(t)) dt. \tag{3.35}$$

From (3.35), we have that

$$x(t_{r+1}) - x(t_r) = \frac{(1-\theta)}{N(\theta)} \big(y(t_r, x(t_r)) - y(t_{r-1}, x(t_{r-1}))\big) + \frac{\theta}{N(\theta)} \int_{t_r}^{t_{r+1}} y(t, x(t))\, dt, \tag{3.36}$$

where

$$\begin{aligned}\int_{t_r}^{t_{r+1}} y\left(t, x\left(t\right)\right) dt =& \int_{t_r}^{t_{r+1}} \left[\frac{y\left(t_r, x_r\right)}{p}\left(t - t_{r-1}\right) - \frac{y\left(t_{r-1}, x_{r-1}\right)}{p}\left(t - t_r\right)\right] \\ =& \frac{3P}{2} y\left(t_r, x_n\right) - \frac{P}{2} y\left(t_{r-1}, x_{r-1}\right).\end{aligned} \tag{3.37}$$

From equation (3.36), the following solution is obtained

$$\begin{aligned}x\left(t_{r+1}\right) - x\left(t_r\right) =& \frac{\left(1-\theta\right)}{N\left(\theta\right)}\left[\left(y\left(t_r, x\left(t_r\right)\right) - y(t_{r-1}, x\left(t_{r-1}\right)\right)\right] \\ &+ \frac{\theta}{N\left(\theta\right)}\left[\frac{3P}{2} y\left(t_r, x\left(t_r\right)\right) - \frac{P}{2} y\left(t_{r-1}, x\left(t_{r-1}\right)\right)\right].\end{aligned} \tag{3.38}$$

Therefore,

$$\begin{aligned}x\left(t_{r+1}\right) - x\left(t_r\right) =& \left(\frac{\left(1-\theta\right)}{N\left(\theta\right)} + \frac{3\theta P}{2N\left(\theta\right)}\right) y\left(t_r, x\left(t_r\right)\right) \\ &- \left(\frac{\left(1-\theta\right)}{N\left(\theta\right)} + \frac{\theta P}{2N\left(\theta\right)}\right) y\left(t_{r-1}, x\left(t_{r-1}\right)\right).\end{aligned} \tag{3.39}$$

Equation (3.39) has the solution of the form

$$\begin{aligned}x\left(_{r+1}\right) - x\left(_r\right) =& \left(\tfrac{\left(1-\theta\right)}{N\left(\theta\right)} + \tfrac{3\theta P}{2N\left(\theta\right)}\right) y\left(_r, x\left(t_r\right)\right) \\ &- \left(\tfrac{\left(1-\theta\right)}{N\left(\theta\right)} + \tfrac{\theta P}{2N\left(\theta\right)}\right) y\left(t_{r-1}, x\left(t_{r-1}\right)\right).\end{aligned} \tag{3.40}$$

This is the two-step Adams-Bashforth-Moulton numerical method for the Caputo-Fabrizio fractional order derivative.

3.4. Caputo-Fabrizio derivative COVID-19 model numerical method

We now employ the above two-step Adams-Bashforth-Moulton numerical algorithm proposed to obtain the approximate solution of model (2.4).

$$\begin{aligned}S_{r+1} =& S_r + \left(\tfrac{\left(1-\theta\right)}{N\left(\theta\right)} + \tfrac{3\theta P}{2N\left(\theta\right)}\right) y_1\left(t_r, S_r, E_r, Q_r, I_{Tr}, R_r\right) \\ &- \left(\tfrac{\left(1-\theta\right)}{N\left(\theta\right)} + \tfrac{\theta P}{2N\left(\theta\right)}\right) y_1\left(t_{r-1}, S_{r-1}, E_{r-1}, Q_{r-1}, I_{Tr-1}, R_{r-1}\right), \\ E_{r+1} =& E_r + \left(\tfrac{\left(1-\theta\right)}{N\left(\theta\right)} + \tfrac{3\theta P}{2N\left(\theta\right)}\right) y_2\left(t_r, S_r, E_r, Q_r, I_{Tr}, R_r\right) \\ &- \left(\tfrac{\left(1-\theta\right)}{N\left(\theta\right)} + \tfrac{\theta P}{2N\left(\theta\right)}\right) y_2\left(t_{r-1}, S_{r-1}, E_{r-1}, Q_{r-1}, I_{Tr-1}, R_{r-1}\right), \\ Q_{r+1} =& Q_r + \left(\tfrac{\left(1-\theta\right)}{N\left(\theta\right)} + \tfrac{3\theta P}{2N\left(\theta\right)}\right) y_3\left(t_r, S_r, E_r, Q_r, I_{Tr}, R_r\right) \\ &- \left(\tfrac{\left(1-\theta\right)}{N\left(\theta\right)} + \tfrac{\theta P}{2N\left(\theta\right)}\right) y_3\left(t_{r-1}, S_{r-1}, E_{r-1}, Q_{r-1}, I_{Tr-1}, R_{r-1}\right), \\ I_{Tr+1} =& I_{Tr} + \left(\tfrac{\left(1-\theta\right)}{N\left(\theta\right)} + \tfrac{3\theta P}{2N\left(\theta\right)}\right) y_4\left(t_r, S_r, E_r, Q_r, I_{Tr}, R_r\right) \\ &- \left(\tfrac{\left(1-\theta\right)}{N\left(\theta\right)} + \tfrac{\theta P}{2N\left(\theta\right)}\right) y_4\left(t_{r-1}, S_{r-1}, E_{r-1}, Q_{r-1}, I_{Tr-1}, R_{r-1}\right), \\ R_{r+1} =& R_r + \left(\tfrac{\left(1-\theta\right)}{N\left(\theta\right)} + \tfrac{3\theta P}{2N\left(\theta\right)}\right) y_5\left(t_r, S_r, E_r, Q_r, I_{Tr}, R_r\right) \\ &- \left(\tfrac{\left(1-\theta\right)}{N\left(\theta\right)} + \tfrac{\theta P}{2N\left(\theta\right)}\right) y_5\left(t_{r-1}, S_{r-1}, E_{r-1}, Q_{r-1}, I_{Tr-1}, R_{r-1}\right).\end{aligned} \tag{3.41}$$

4. Adams-type predictor corrector numerical method with Atagana-Baleanu-derivative fractional order model

In this section, we employ the Adams-type predictor corrector numerical method used [54] to obtain an approximate solution of our COVID-19 model (2.5).

Recall that our COVID-19 model in the sense of Atagana-Baleanu-derivative with the generalized Mittag-Leffler function is given as:

$$\left.\begin{aligned}
{}_0^{ABC}D_t^{\theta}S(t) &= \Lambda - \beta_1 SE - \beta_2 SI_T + \lambda Q + \omega R - \mu S,\\
{}_0^{ABC}D_t^{\theta}E(t) &= \beta_1 SE + \beta_2 SI_T - \alpha_1 E - \tau E - \mu E,\\
{}_0^{ABC}D_t^{\theta}Q(t) &= \tau E - \lambda Q - \alpha_2 Q - \mu Q,\\
{}_0^{ABC}D_t^{\theta}I_T(t) &= \alpha_1 E + \alpha_2 Q - \phi I_T - \sigma I_T - \mu I_T,\\
{}_0^{ABC}D_t^{\theta}R(t) &= \phi I_T - \omega R - \mu R.
\end{aligned}\right\}$$

This can also be written as:

$$\left.\begin{aligned}
{}_0^{ABC}D_t^{\theta}S(t) &= y_1(t,S,E,Q,I_T,R),\\
{}_0^{ABC}D_t^{\theta}E(t) &= y_2(t,S,E,Q,I_T,R),\\
{}_0^{ABC}D_t^{\theta}Q(t) &= y_3(t,S,E,Q,I_T,R),\\
{}_0^{ABC}D_t^{\theta}I_T(t) &= y_4(t,S,E,Q,I_T,R),\\
{}_0^{ABC}D_t^{\theta}R(t) &= y_5(t,S,E,Q,I_T,R).
\end{aligned}\right\} \tag{4.1}$$

Applying the Atagana-Baleanu (AB) fractional order integral on both sides of the equation.

$$\begin{aligned}
S(t) &= S_0(t) + \frac{(1-\theta)}{AB(\theta)}y_1(t,S,E,Q,I_T,R) + \frac{\theta}{AB\left|\overline{(\theta)}\right|}\int_0^t y_1(t,S,E,Q,I_T,R)(t-\psi)^{\theta-1}d\psi,\\
E(t) &= E_0(t) + \frac{(1-\theta)}{AB(\theta)}y_2(t,S,E,Q,I_T,R) + \frac{\theta}{AB\left|\overline{(\theta)}\right|}\int_0^t y_2(t,S,E,Q,I_T,R)(t-\psi)^{\theta-1}d\psi,\\
Q(t) &= Q_0(t) + \frac{(1-\theta)}{AB(\theta)}y_3(t,S,E,Q,I_T,R) + \frac{\theta}{AB\left|\overline{(\theta)}\right|}\int_0^t y_3(t,S,E,Q,I_T,R)(t-\psi)^{\theta-1}d\psi,\\
I_T(t) &= I_{T0}(t) + \frac{(1-\theta)}{AB(\theta)}y_4(t,S,E,Q,I_T,R) + \frac{\theta}{AB\left|\overline{(\theta)}\right|}\int_0^t y_4(t,S,E,Q,I_T,R)(t-\psi)^{\theta-1}d\psi,\\
R(t) &= R_0(t) + \frac{(1-\theta)}{AB(\theta)}y_5(t,S,E,Q,I_T,R) + \frac{\theta}{AB\left|\overline{(\theta)}\right|}\int_0^t y_5(t,S,E,Q,I_T,R)(t-\psi)^{\theta-1}d\psi.
\end{aligned} \tag{4.2}$$

To investigate the above fractional order integral numerically, we therefore approximate the fractional order integral numerically. Employing the Adams-type predictor-corrector method presented in [54] for Atagana-Baleanu fractional integral, we now have

$$ {}_{0}^{AB}I_{t}^{\theta}\left[x\left(t\right)\right]=\frac{1-\theta}{AB\left(\theta\right)}x\left(t\right)+\frac{\theta}{AB\left(\theta\right)\left|\overline{\left(\theta\right)}\right.}\int_{0}^{t}x\left(\psi\right)\left(t-\psi\right)^{\theta-1}d\psi. \tag{4.3} $$

by letting $P=\frac{T}{N},t_{r}=rp,(r=0,1,2,3,...R)$.

We therefore consider the solution in the interval of $[0,T]$.

Therefore the corrector formula for the Atagana-Baleanu fractional-integral version is presented as:

$$ \begin{aligned} x_{p}\left(t_{r+1}\right)&=x_{0}\left(t_{r+1}\right)+\tfrac{(1-\theta)P^{\theta}}{AB(\theta)\left|\overline{(\theta+2)}\right.}y\left(t_{r+1},x_{p}^{V}\left(t_{r+1}\right)\right)\\ &+\tfrac{\theta P^{\theta}}{AB(\theta)\left|\overline{(\theta+2)}\right.}\sum_{i=0}^{k}\Upsilon_{i,r+1}y\left(t_{i},x_{p}\left(t_{i}\right)\right), \end{aligned} $$

where

$$ \Upsilon_{i,r+1}=\begin{cases} r^{\theta+1}-\left(r-\theta\right)\left(r+1\right)^{\theta},if\,i=0,\\ \left(r-i+2\right)^{\theta+1}+\left(r-i\right)^{\theta+1}-2(r-i+1)^{\theta+1},1\leq i\leq r,\\ 1i=r+1. \end{cases} $$

Similarly, the predictor $x^{V}\left(t_{r+1}\right)$ is expressed as given below:

$$ \begin{aligned} x_{P}^{V}\left(t_{r+1}\right)&=x_{0}+\tfrac{(1-\theta)}{AB(\theta)}y\left(t_{r},x_{P}\left(t_{r}\right)\right)\\ &+\tfrac{\theta}{AB(\theta)\left|\overline{(\theta)^{2}}\right.}\sum_{i=0}^{k}\Delta_{i,r+1}y\left(t_{i},x_{p}\left(t_{i}\right)\right), \end{aligned} $$

where

$$ \Delta_{i,r+1}=\frac{P^{\theta}}{\theta}\left(\left(r+1-i\right)^{\theta}-\left(r-i\right)^{\theta}\right),0\leq i\leq r. $$

We therefore present our model (2.5) as given in (4.4) using the Adam-type predictor-

corrector numerical method.

$$
\begin{aligned}
S_{r+1} &= S(0) + \frac{(1-\theta)P^{\theta}}{AB(\theta)\lceil(\theta+2)} \begin{bmatrix} y_1\left(t_{r+1}, S^V_{r+1}, E^V_{r+1}, Q^V_{r+1}, I^V_{Tr+1}, R^V_{r+1}\right) \\ + \frac{\theta P^{\theta}}{AB(\theta)\lceil(\theta+2)} \sum_{i=0}^{k} \Upsilon_{i,r+1} y_1(t_i, S_i, E_i, Q_i, I_{Ti}, R_i) \end{bmatrix}, \\
E_{r+1} &= E(0) + \frac{(1-\theta)P^{\theta}}{AB(\theta)\lceil(\theta+2)} \begin{bmatrix} y_2\left(t_{r+1}, S^V_{r+1}, E^V_{r+1}, Q^V_{r+1}, I^V_{Tr+1}, R^V_{r+1}\right) \\ + \frac{\theta P^{\theta}}{AB(\theta)\lceil(\theta+2)} \sum_{i=0}^{k} \Upsilon_{i,r+1} y_1(t_i, S_i, E_i, Q_i, I_{Ti}, R_i) \end{bmatrix}, \\
Q_{r+1} &= Q(0) + \frac{(1-\theta)P^{\theta}}{AB(\theta)\lceil(\theta+2)} \begin{bmatrix} y_3\left(t_{r+1}, S^V_{r+1}, E^V_{r+1}, Q^V_{r+1}, I^V_{Tr+1}, R^V_{r+1}\right) \\ + \frac{\theta P^{\theta}}{AB(\theta)\lceil(\theta+2)} \sum_{i=0}^{k} \Upsilon_{i,r+1} y_1(t_i, S_i, E_i, Q_i, I_{Ti}, R_i) \end{bmatrix}, \\
I_{Tr+1} &= I_T(0) + \frac{(1-\theta)P^{\theta}}{AB(\theta)\lceil(\theta+2)} \begin{bmatrix} y_3\left(t_{r+1}, S^V_{r+1}, E^V_{r+1}, Q^V_{r+1}, I^V_{Tr+1}, R^V_{r+1}\right) \\ + \frac{\theta P^{\theta}}{AB(\theta)\lceil(\theta+2)} \sum_{i=0}^{k} \Upsilon_{i,r+1} y_1(t_i, S_i, E_i, Q_i, I_{Ti}, R_i) \end{bmatrix}, \\
R_{r+1} &= R(0) + \frac{(1-\theta)P^{\theta}}{AB(\theta)\lceil(\theta+2)} \begin{bmatrix} y_4\left(t_{r+1}, S^V_{r+1}, E^V_{r+1}, Q^V_{r+1}, I^V_{Tr+1}, R^V_{r+1}\right) \\ + \frac{\theta P^{\theta}}{AB(\theta)\lceil(\theta+2)} \sum_{i=0}^{k} \Upsilon_{i,r+1} y_1(t_i, S_i, E_i, Q_i, I_{Ti}, R_i) \end{bmatrix},
\end{aligned} \tag{4.4}
$$

where $S^V_{r+1}, E^V_{r+1}, Q^V_{r+1}, I^V_{Tr+1}, R^V_{r+1}$ are the predictors given as:

$$
\begin{aligned}
S^V_{r+1} &= S(0) + \frac{(1-\theta)}{AB(\theta)} y_1(t_r, S_r, E_r, Q_r, I_{Tr}, R_r) + \frac{\theta}{\left|\overline{(\theta)}\right|^2 AB(\theta)} \sum_{i=0}^{k} \Delta_{i,k+1} y_1(t_i, S_i, E_i, Q_i, I_{Ti}, R_i), \\
E^V_{r+1} &= E(0) + \frac{(1-\theta)}{AB(\theta)} y_2(t_r, S_r, E_r, Q_r, I_{Tr}, R_r) + \frac{\theta}{\left|\overline{(\theta)}\right|^2 AB(\theta)} \sum_{i=0}^{k} \Delta_{i,k+1} y_2(t_i, S_i, E_i, Q_i, I_{Ti}, R_i), \\
Q^V_{r+1} &= Q(0) + \frac{(1-\theta)}{AB(\theta)} y_3(t_r, S_r, E_r, Q_r, I_{Tr}, R_r) + \frac{\theta}{\left|\overline{(\theta)}\right|^2 AB(\theta)} \sum_{i=0}^{k} \Delta_{i,k+1} y_3(t_i, S_i, E_i, Q_i, I_{Ti}, R_i), \\
I^V_{Tr+1} &= I_T(0) + \frac{(1-\theta)}{AB(\theta)} y_4(t_r, S_r, E_r, Q_r, I_{Tr}, R_r) + \frac{\theta}{\left|\overline{(\theta)}\right|^2 AB(\theta)} \sum_{i=0}^{k} \Delta_{i,k+1} y_4(t_i, S_i, E_i, Q_i, I_{Ti}, R_i), \\
R^V_{r+1} &= R(0) + \frac{(1-\theta)}{AB(\theta)} y_5(t_r, S_r, E_r, Q_r, I_{Tr}, R_r) + \frac{\theta}{\left|\overline{(\theta)}\right|^2 AB(\theta)} \sum_{i=0}^{k} \Delta_{i,k+1} y_5(t_i, S_i, E_i, Q_i, I_{Ti}, R_i).
\end{aligned} \tag{4.5}
$$

4.1. Fractional order COVID-19 model simulation

In this section, we present the numerical simulation of the COVID-19 model employing the three differential operators used. The values of our model variable(parameters) used for this simulation are presented in Tables (1) and (2) below.

Variables (Parameters)	Description	Values/day	Sources
S	Susceptible individuals	100	[30]
E	Exposed individuals	70	Estimated
Q	Quarantined individuals	50	Estimated
I_T	Infected but isolated for treatment	20	Estimated
R	Recovered individuals	10	Estimated
Λ	Recruitment rate	400	[58]
β_1	Contact rate of S and E	0.3	[55]
β_2	Contact rate of S and I_T	0.4	[58]
λ	Rate at which the quarantined becomes susceptible	0.05	Estimated

Table 1. Description of Variables and Parameters

Variables (Parameters)	Description	Values/day	Sources
ω	Rate at which the recovered becomes susceptible	0.001	Estimated
α_1	Rate at which the exposed becomes infectious and taken for treatment	0.35	[56]
α_2	Rate at which the quarantined who develops symptoms and are taken for treatment	0.45	[30]
Υ	Rate at which the exposed are quarantined for diagnosis	0.003	[57]
ϕ	Rate at which those treated recovered	0.1	Estimated
σ	COVID-19 disease induced death rate	0.002	[58]
μ	Natural death rate	0.0005	[58]

Table 2. Description of Variables and Parameters

The multifaceted depiction of all compartments − Susceptible (S), Exposed (E), Quarantined (Q), Isolated for Treatment (I_T), and Recovered (R) − presented on a single graph, while varying the fractional order (θ), offers a comprehensive exploration of the epidemic's dynamics under differing memory effects. As θ is increased to 0.95 as observed in Figures (2(a)),(6(a)) and (10(a)), the epidemic response

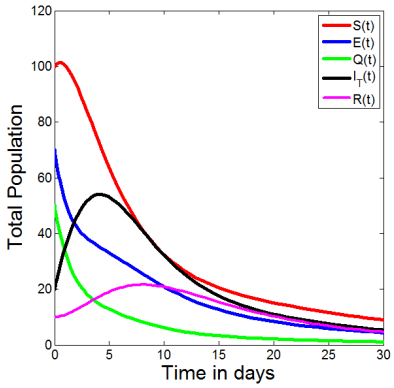

(a) Behaviors of the system (2.3) by adopting Caputo derivative for $\theta = 0.95$

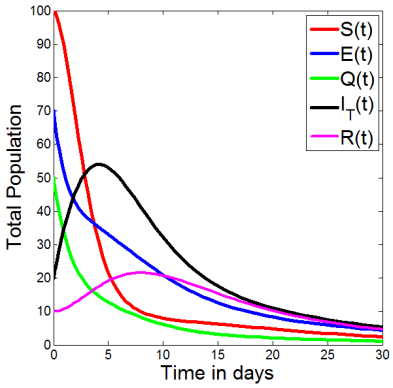

(b) Behaviors of the system (2.3) by adopting Caputo derivative for $\theta = 0.85$

Figure 2. Total Human Population

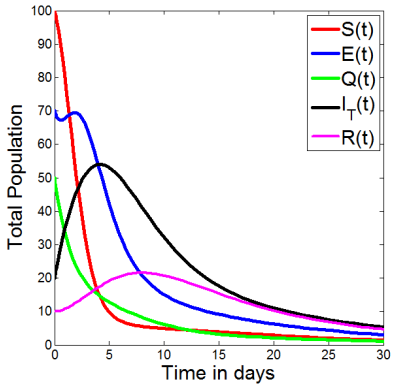

(a) Behaviors of the system (2.3) by adopting Caputo derivative for $\theta = 0.75$

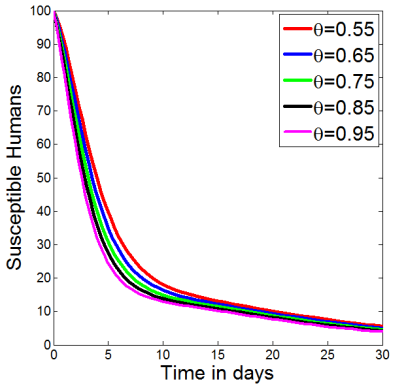

(b) The plot for the Susceptible population for Caputo derivative

Figure 3. Human Population

is characterized by a substantial memory influence, engendering smoother transitions between compartments. This manifests as a gradual ascent and decline of each population, effectively elongating the outbreak's duration and tempering the zenith of infections. The pronounced memory effect facilitates a more discernible progression of the epidemic, allowing for more measured responses and potentially enhanced management of healthcare resources. This enables healthcare systems to anticipate and allocate resources such as hospital beds, medical supplies, and healthcare personnel more effectively over time, preventing sudden surges that overwhelm the system. However, this smoother trajectory might also imply a prolonged period of susceptibility and a more protracted recovery phase as the epidemic wanes. Conversely, when θ diminishes to 0.85 as observed in Figures (2(b)),(6(b)) and (10(b)), the memory effect weakens, precipitating sharper transitions between compartments. This intensifies the initial surge of exposed and quarantined individuals, suggesting a potentially more rapid transmission and response dynamics. The sharp

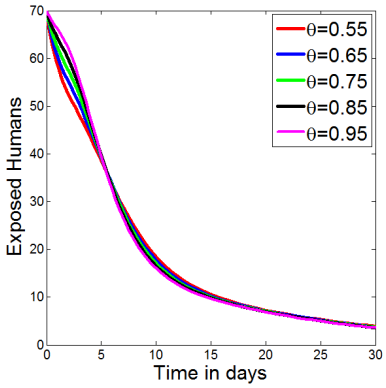

(a) The plot for the Exposed population for Caputo derivative

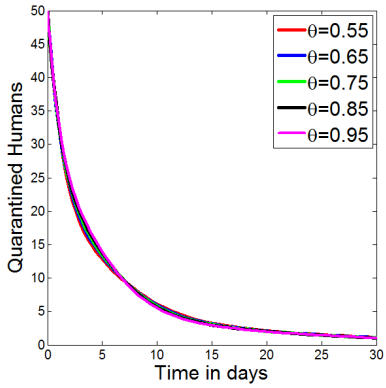

(b) The plot for the Quarantined population for Caputo derivative

Figure 4. Human Population

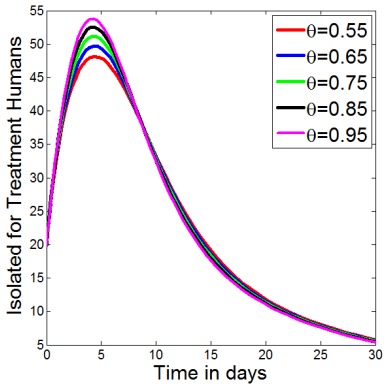

(a) The plot for the Isolated population for Caputo derivative

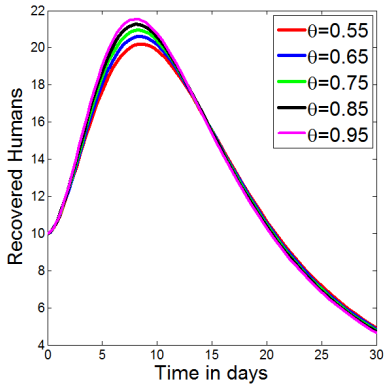

(b) The plot for the Recovered population for Caputo derivative

Figure 5. Human Population

rise indicates that interventions like quarantining or isolation must be implemented promptly to prevent rapid virus transmission. This surge also underscores the urgency of enforcing social distancing or other immediate measures. The accelerated rise in these populations might reflect a more urgent need for containment measures and resource allocation to curb the spread of the disease. However, despite these intensified efforts, the isolated for treatment population experiences a delayed peak, indicating an extended strain on healthcare infrastructure. This delayed peak underscores the complexities of managing the epidemic, necessitating sustained vigilance and adaptable healthcare systems to address evolving demands. Although the initial phases may show sharp increases, the delayed peak for the treated population indicates that hospitals will face sustained pressure over an extended period, necessitating consistent preparedness and effective resource management. Notably, amidst these variations in θ, the recovered population exhibits a consistent upward trajectory, illustrating the enduring progression of immunity within the population. This

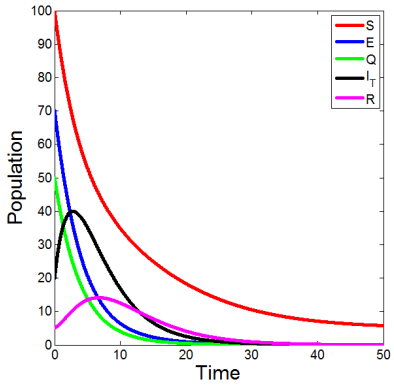

(a) Behaviors of the system (2.4) by adopting Caputo-Fabrizio derivative for $\theta = 0.95$

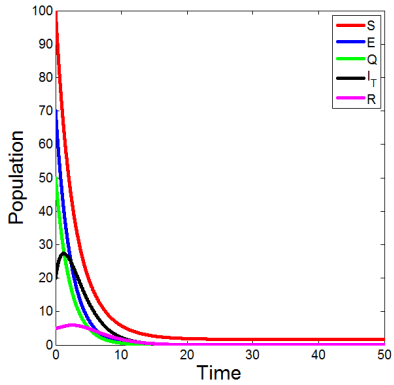

(b) Behaviors of the system (2.4) by adopting Caputo-Fabrizio derivative for $\theta = 0.85$

Figure 6. Human Population

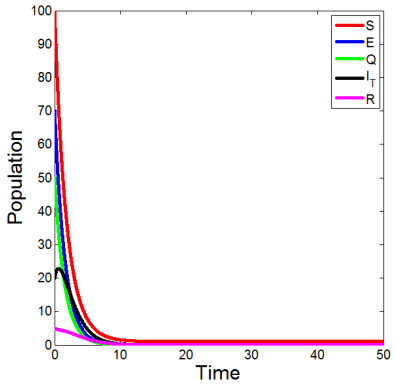

(a) Behaviors of the system (2.4) by adopting Caputo-Fabrizio derivative for $\theta = 0.75$

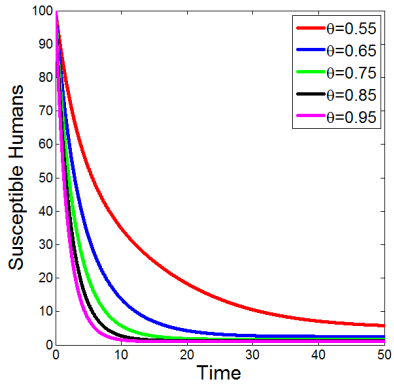

(b) The plot for the Susceptible population for Caputo-Fabrizio derivative

Figure 7. Human Population

resilience in the recovered population underscores the potential for long-term immunity and serves as a beacon of hope amidst the challenges posed by the epidemic. The intricate interplay between θ variations and epidemic dynamics using the three different differential fractional order operators unveils a spectrum of scenarios, each presenting unique challenges and opportunities for public health intervention. These insights are invaluable for guiding public health policies, as they enable flexibility in strategies based on disease progression. Slower dynamics prioritize long-term public health interventions, while faster dynamics require immediate containment measures. These insights gleaned from the comprehensive analysis of all compartments on a single graph serve as a valuable guide for policymakers, enabling them to tailor interventions, allocate resources judiciously, and foster resilient healthcare systems capable of effectively managing epidemics amidst evolving circumstances.

When these compartments are plotted using different fractional derivative operators − specifically, the fractional Caputo derivative operator, the Caputo-Fabrizio

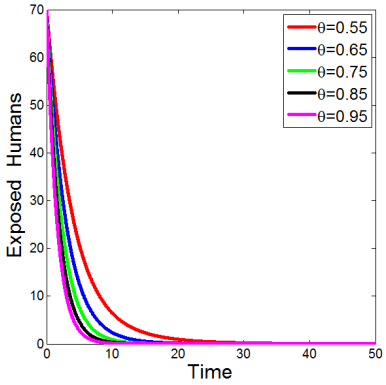

(a) The plot for the Exposed population for Caputo-Fabrizio derivative

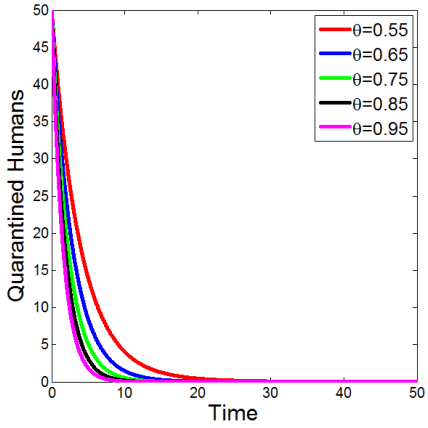

(b) The plot for the Quarantined population for Caputo-Fabrizio derivative

Figure 8. Human Population

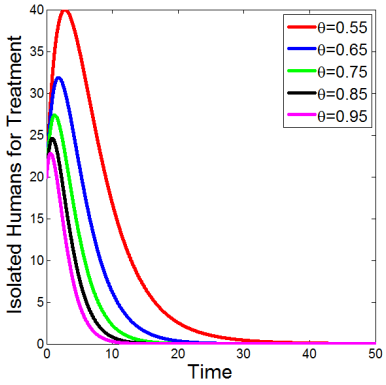

(a) The plot for the Isolated population for Caputo-Fabrizio derivative

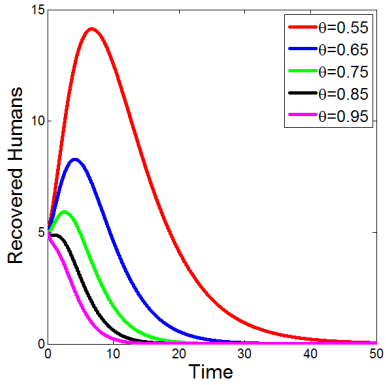

(b) The plot for the Recovered population for Caputo-Fabrizio derivative

Figure 9. Human Population

operator, and the Atagana-Baleanu operator – the resulting graphs offer nuanced insights into the epidemic dynamics. The fractional Caputo derivative operator, known for its widespread application in modeling complex systems with memory effects, captures the gradual transitions between compartments, reflecting the extended duration of the outbreak and the tempered peaks of infections as observed in Figures (3(b)), (4(a)), (4(b)), (5(a)) and (5(b)). This gradual progression indicates a slower spread of infection, where the memory effects of past states influence current infection rates, leading to a more controlled and extended outbreak. Such behavior suggests that interventions can be implemented in a less reactive manner, allowing health systems more time to adapt and allocate resources effectively. Conversely, the Caputo-Fabrizio operator, incorporating a stretched exponential function, provides a more nuanced representation of the COVID-19 epidemic dynamics, potentially revealing subtle variations in the rate of change within each compartment as ob-

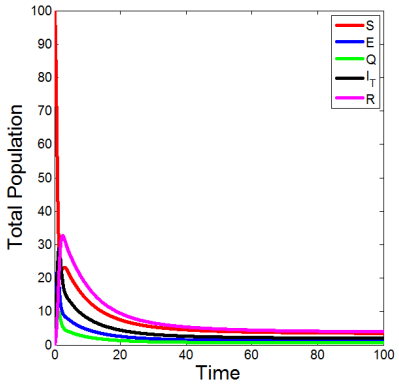

(a) Behaviors of the system (2.5) by adopting Caputo-Fabrizio derivative for $\theta = 0.95$

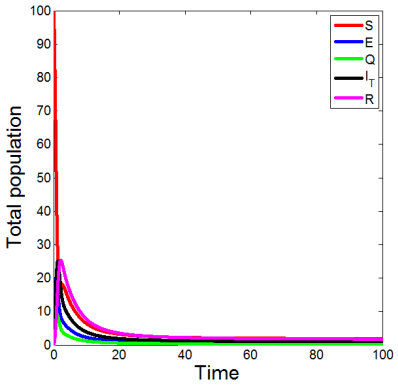

(b) Behaviors of the system (2.5) by adopting Atagana Baleanu derivative for $\theta = 0.85$

Figure 10. Human Population

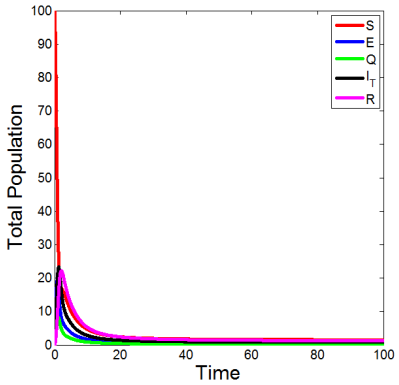

(a) Behaviors of the system (2.5) by adopting Caputo-Fabrizio derivative for $\theta = 0.75$

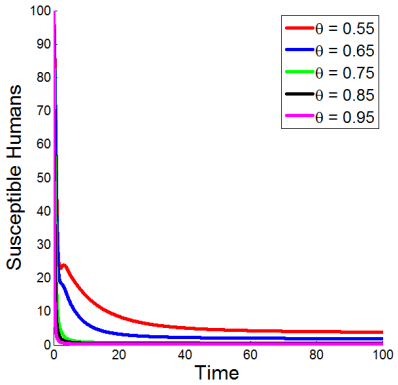

(b) The plot for the Susceptible population for the Atagana Baleanu derivative

Figure 11. Human Population

served in Figures (7(b)), (8(a)), (8(b)), (9(a)) and (9(b)). This operator smooths out abrupt changes, portraying a system where sudden shifts in infection dynamics are less likely, making it suitable for understanding epidemics that display intermediate memory effects. This reflects a more adaptive public health response, as the smoother curve allows for gradual policy changes in response to evolving data. Meanwhile, the Atagana-Baleanu operator, which incorporates a power-law kernel, offers a unique perspective on the epidemic's dynamics, possibly highlighting long-range correlations and non-local effects that influence the spread of the disease as observed in Figures (11(b)), (12(a)), (12(b)), (13(a)) and (13(b)). The power-law kernel emphasizes the non-local influences, where past states of infection have long-term effects on future disease dynamics. This leads to more prolonged epidemic cycles, where the effects of initial infections reverberate through time, underscoring the need for sustained long-term intervention strategies. The Susceptible Population (S) exhibits a gradual decline over time, reflecting the spread of the disease and

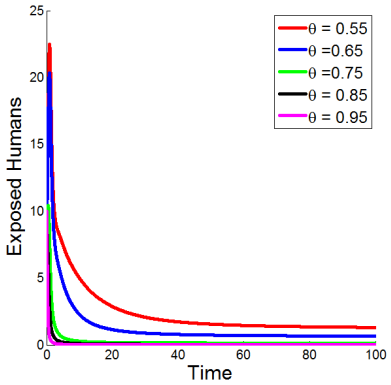

(a) The plot for the Exposed population for the Atagana Baleanu derivative

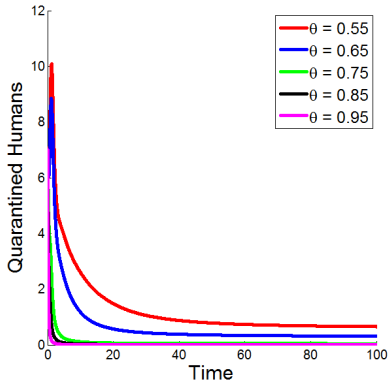

(b) The plot for the Quarantined population for the Atagana Baleanu derivative

Figure 12. Human Population

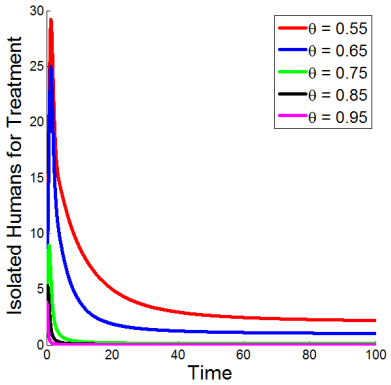

(a) The plot for the Isolated population for the Atagana Baleanu derivative

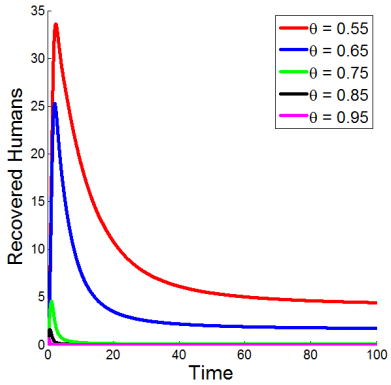

(b) The plot for the Recovered population for the Atagana Baleanu derivative

Figure 13. Human Population

the decrease in susceptible individuals due to infections and natural deaths. When plotted using the fractional Caputo derivative operator, this decline is smooth and gradual, capturing the epidemic's progression. This suggests that as the memory effect increases, the reduction in the susceptible population becomes slower, allowing for a more predictable and gradual exhaustion of susceptible individuals, which provides critical insight into how public health measures can be sustained over longer periods. The Caputo-Fabrizio operator reveals nuanced variations in the decline rate, while the Atagana-Baleanu operator highlights long-range correlations or nonlocal effects influencing susceptibility dynamics. These long-range effects indicate that even past exposures have an extended influence on future susceptibility, meaning that early interventions can have far-reaching consequences on the susceptible population's long-term behavior.

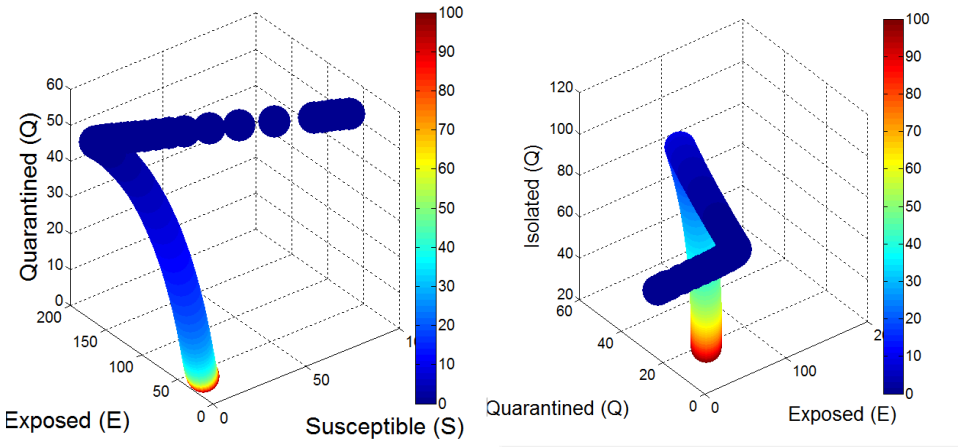

(a) Phase portrait of S, E and Q

(b) Phase portrait of E, Q and I_T

Figure 14. Human Population

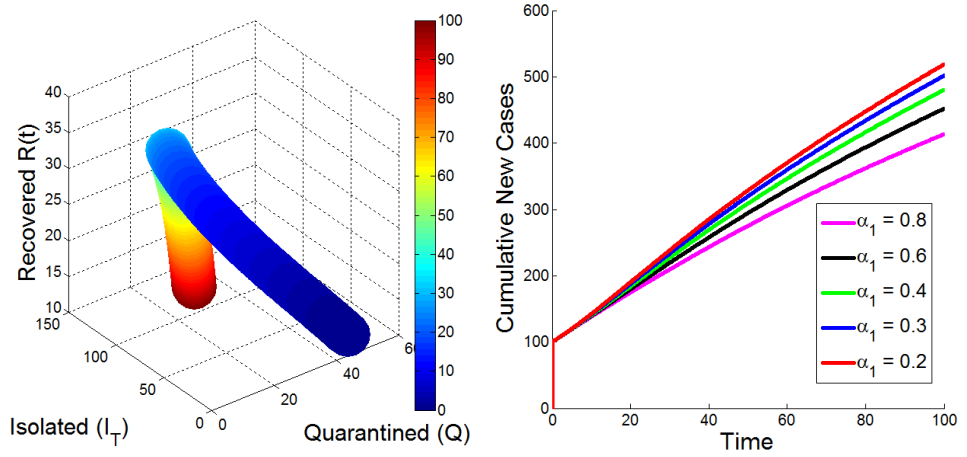

(a) Phase portrait of Q, I_T and R

(b) Effect of varying α_1 on the Cumulative new cases of COVID-19

Figure 15. Human Population

5. Conclusion

In order to comprehend the transmission of disease in a general given population, we have evaluated a variable-order fractional COVID-19 outbreak system in the current study. By using the fractional derivatives of Caputo with power law, Fabrizio with exponential law and Atangana-Baleanu with generalized Mittag-Leffler function the suggested model was made more inclusive.

For a more accurate approximation of the system, three distinct kernels were utilized in the fractional-order derivative operators. A numerical scheme was used to solve the alternative systems: the arbitrary-order Caputo Fabrizio derivative was based on the two-step Adams-Bashforth method, the Atangana-Baleanu frac-

tional derivative was based on the Adams type predictor-corrector, and the Caputo fractional derivative was based on the Adams-Bashforth-Moulton scheme. Additionally, the current investigation's use of fixed-point theory supported the need for the fractional-order system for the Caputo Fabrizio to have the presence of a unique solution. We also observed from the graphs of our numerical simulations that increasing the fractional order (memory effect) generally leads to a slower progression of the disease, reflecting the memory effect inherent in fractional derivatives. Specifically, higher values of the fractional order correspond to a more gradual spread, reducing the peak number of infections and spreading the cases over a longer period, as seen in the dynamics of the population of the Isolated for treatment class depicted in Figures (5(a)), (9(a)), and (13(a)). Our graphical representations investigate the efficiency and dependability of the suggested methods. The impacts of the different arbitrary-order values have been examined and are shown graphically in a number of figures.

The results indicate that quarantine and isolation for treatment measures significantly impact the transmission dynamics of COVID-19. Increasing the rate of isolation of infected individuals α_1 leads to a notable decrease in the cumulative number of new cases. This is attributed to the prompt removal of infected individuals from the general population, reducing the contact rate between infected and susceptible individuals and thereby slowing the spread of the virus. Similarly, effective quarantine measures that quickly identify and isolate exposed individuals before they become infectious can substantially reduce the overall transmission rate. The graphs clearly demonstrate that higher rates of quarantine and isolation result in lower peaks of infections and a faster decline in new cases, highlighting the importance of these interventions in controlling the outbreak. These findings underscore the critical role of timely and effective quarantine and isolation strategies in mitigating the impact of infectious disease outbreaks.

In summary, the model dynamics are better explained by the arbitrary-order derivative operators that were applied.

Direction for future research

Future research could expand on this work by addressing the challenges studied in the novel trial functions and rogue waves of the generalized breaking soliton equation, using the bilinear neural network method developed by Zhang et al. as presented in [59].

Credit authorship contribution Statement

William Atokolo: Writing original draft, formal analysis.
Remegius Okeke Aja: Writing and editing.
David Omale: Supervision.
Godwin Onuche Acheneje: Formal Analysis and Simulation.
Rose Veronica Paul: Review and Editing.
Jeremiah Amos: Review and Editing.

Declaration of Competing Interest

The authors declare that they have no known competing interests.

Data Availability

Values of parameters used are adequately cited and referenced.

Acknowledgments

The authors would like to thank the editors and anonymous reviewers for their valuable suggestions.

References

[1] S. Kumar, S. Ghosh, R. Kumar, M. Jleli, *A fractional model for population dynamics of two interacting species by using spectral and Hermite wavelets methods*, Numer. Methods Partial Differential Equations, 2020.
DOI: 10.1002/num.22602

[2] S. Kumar, R. Kumar, M. S. Osman, B. Samet, *A wavelet based numerical scheme for fractional order SEIR epidemic of measles by using Genocchi polynomials*, Numer. Methods Partial Differential Equations, 2020.
DOI: 10.1002/num.22577

[3] K. A. Abro and A. Atangana, *A comparative study of convective fluid motion in rotating cavity via Atangana-Baleanu and Caputo-Fabrizio fractal-fractional differentiations*, Eur. Phys. J. Plus 135, 2020.
DOI: 10.1140/epjp/s13360-020-00136-x

[4] M. Al-Refai and T. Abdeljawad, *Analysis of the fractional diffusion equations with fractional derivative of non-singular kernel*, Adv. Difference Equ. 2017, 2017.
DOI: 10.1186/s13662-017-1356-2

[5] B. Ghanbari, S. Kumar, and R. Kumar, *A study of behaviour for immune and tumor cells in immunogenetic tumour model with non-singular fractional derivative*, Chaos Solitons Fractals 133, 2020.
DOI: 10.1016/j.chaos.2020.109619

[6] S. Kumar, *A new analytical modelling for fractional telegraph equation via Laplace transform*, Appl. Math. Model. 38, 2014.
DOI: 10.1016/j.apm.2013.11.035

[7] B. B. Mandelbrot and J. W. Van Ness, *Fractional Brownian motions, fractional noises and applications*, SIAM Rev. 10, 1968.

[8] M. Pakdaman, A. Ahmadian, S. Effati, S. Salahshour, D. Baleanu, *Solving differential equations of fractional order using an optimization technique based on training artificial neural network*, Appl. Math. Comput. 293, 2017.
DOI: 10.1016/j.amc.2016.07.021

[9] S. Salahshour, A. Ahmadian, M. Salimi, M. Ferrara, D. Baleanu, *Asymptotic solutions of fractional interval differential equations with nonsingular kernel derivative*, Chaos 29, 2019.
DOI: 10.1063/1.5096022

[10] I. Podlubny, *Fractional differential equations: An introduction to fractional derivatives, fractional differential equations, to methods of their solution and some of their applications*, Vol. 198, Elsevier, New York, 1998.

[11] A. Atangana and D. Baleanu, *New fractional derivatives with nonlocal and non-singular kernel: theory and application to heat transfer model*, arXiv preprint arXiv:1602.03408, 2016.

[12] M. Caputo and M. Fabrizio, *A new definition of fractional derivative without singular kernel*, Prog. Fract. Differ. Appl. 1, 2015.
DOI: 10.12785/pfda/010201

[13] A. Atangana and J. Gómez-Aguilar, *Fractional derivatives with no-index law property: Application to chaos and statistics*, Chaos Solitons Fractals 114, 2018.
DOI: 10.1016/j.chaos.2018.07.033

[14] H. M. Baskonus and H. Bulut, *On the numerical solutions of some fractional ordinary differential equations by fractional Adams-Bashforth-Moulton method*, Open Math. 13, 2015.
DOI: 10.1515/math-2015-0052

[15] M. A. Dokuyucu and H. Dutta, *A fractional order model for Ebola virus with the new Caputo fractional derivative without singular kernel*, Chaos Solitons Fractals 134, 2020.
DOI: 10.1016/j.chaos.2020.109717

[16] J. Gómez-Aguilar and A. Atangana, *New insight in fractional differentiation: Power, exponential decay and Mittag-Leffler laws and applications*, Eur. Phys. J. Plus 132, 2017.
DOI: 10.1140/epjp/i2017-11293-3

[17] K. Kachia, J. Solís-Pérez, and J. Gómez-Aguilar, *Chaos in a three-cell population cancer model with variable-order fractional derivative with power, exponential and Mittag-Leffler memories*, Chaos Solitons Fractals 140, 2020.
DOI: 10.1016/j.chaos.2020.110177

[18] K. M. Owolabi, J. Gómez-Aguilar, and B. Karaagac, *Modelling, analysis and simulations of some chaotic systems using derivative with Mittag-Leffler kernel*, Chaos Solitons Fractals 125, 2019.
DOI: 10.1016/j.chaos.2019.05.019

[19] S. Qureshi and A. Yusuf, *Modeling chickenpox disease with fractional derivatives: From Caputo to Atangana-Baleanu*, Chaos Solitons Fractals 122, 2019.
DOI: 10.1016/j.chaos.2019.03.020

[20] B. S. T. Alkahtani, *Chua's circuit model with Atangana-Baleanu derivative with fractional order*, Chaos Solitons Fractals 89, 2016.
DOI: 10.1016/j.chaos.2016.03.020

[21] A. Arikoglu and I. Ozkol, *Solution of fractional differential equations by using differential transform method*, Chaos Solitons Fractals 34, 2007.
DOI: 10.1016/j.chaos.2006.09.004

[22] A. Atangana and S. I. Araz, *New numerical method for ordinary differential equations: Newton polynomial*, J. Comput. Appl. Math. 372, 2020.
DOI: 10.1016/j.cam.2020.112622

[23] A. Atangana and K. M. Owolabi, *New numerical approach for fractional differential equations*, Math. Model. Nat. Phenom. 13, 2018.
DOI: 10.1051/mmnp/2018010

[24] K. Diethelm, and N.J. Ford, *Analysis of Fractional Differential Equations. Journal of Mathematical Analysis and Applications*, 265, 229–248. 2002.
DOI: 10.1006/jmaa.2000.7194

[25] A. Al-khedhairi, A. Elsadany, and A. Elsonbaty, *Modelling immune systems based on Atangana–Baleanu fractional derivative*, Chaos Solitons Fractals, 129, 25–39. 2019.
DOI: 10.1016/j.chaos.2019.07.053

[26] A. Jajarmi and D. Baleanu, *A new fractional analysis on the interaction of HIV with CD4+ T-cells*, Chaos Solitons Fractals 113, 2018.
DOI: 10.1016/j.chaos.2018.06.009

[27] E. Okyere, S. Olaniyi, and E. Bonyah, *Analysis of Zika virus dynamics with sexual transmission route using multiple optimal controls*, Sci. Afr. 9, 2020.
DOI: 10.1016/j.sciaf.2020.e00532

[28] A. S. Shaikh and K. S. Nisar, *Transmission dynamics of fractional order typhoid fever model using Caputo-Fabrizio operator*, Chaos Solitons Fractals 128, 2019.
DOI: 10.1016/j.chaos.2019.08.012

[29] S. Ullah, M. A. Khan, and M. Farooq, *A fractional model for the dynamics of TB virus*, Chaos Solitons Fractals 116, 2018.
DOI: 10.1016/j.chaos.2018.09.001

[30] S. Kumar, R. P. Chauhan, S. Momani, S. Hadid, *Investigations on COVID-19 model through singular and non-singular fractional operators*, Numer. Methods Partial Differential Eq., 2020.
DOI: 10.1002/num.22707

[31] W. Atokolo, R. O. Aja, S. E. Aniaku, I. S. Onah, G. C. E. Mbah, *Approximate solution of the fractional order sterile insect technology model via the Laplace Adomian decomposition method for the spread of Zika virus disease*, Int. J. Math. Math. Sci., 2022.
DOI: 10.1155/2022/2297630

[32] W. Atokolo, R. O. Aja, D. Omale, Q. O. Ahmon, G. O. Acheneje, J. Amos, *Fractional mathematical model for the transmission dynamics and control of Lassa fever*, Franklin Open, 2024.
DOI: 10.1016/j.fraope.2024.100110

[33] A. Atangana, *Modelling the spread of COVID-19 with new fractal-fractional operators: Can the lockdown save mankind before vaccination?*, Chaos Solitons Fractals 136, 2020.
DOI: 10.1016/j.chaos.2020.109860

[34] T. M. Chen, J. Rui, Q.P. Wang, Z.Y. Zhao, J.A. Cui, L.A. Yin, *A mathematical model for simulating the phase-based transmissibility of a novel coronavirus*, Infect. Dis. Poverty 9, 2020.
DOI: 10.1186/s40249-020-00640-3

[35] M. A. Khan and A. Atangana, *Modeling the dynamics of novel coronavirus (2019-ncov) with fractional derivative*, Alex. Eng. J. 59, 2020.
DOI: 10.1016/j.aej.2020.02.033

[36] C. Yang and J. Wang, *A mathematical model for the novel coronavirus epidemic in Wuhan, China*, Math. Biosci. Eng. 17, 2020.
DOI: 10.3934/mbe.2020148

[37] A. Zeb, E. Alzahrani,V.S. Erturk, G. Zaman, *Mathematical model for coronavirus disease 2019 (COVID-19) containing isolation class*, Biomed. Res. Int.

2020, 2020.
DOI: 10.1155/2020/3452402

[38] Z. Zhang, R. Gul, and A. Zeb, *Global sensitivity analysis of COVID-19 mathematical model*, Alex. Eng. J., 2020.
DOI: 10.1016/j.aej.2020.09.035

[39] M.A. Khan, S. Ullah, S. Kumar, *A robust study on 2019-nCOV outbreaks through non-singular derivative*, Eur. Phys. J. Plus 136, 2021.
DOI: 10.1140/epjp/s13360-021-01159-8

[40] S. Kumar, R.P. Chauhan, S. Momani, S. Hadid, *Numerical investigations on COVID-19 model through singular and non-singular fractional operators*, Numer. Methods Partial Differential Eq. 40, 2024.
DOI: 10.1002/num.22707

[41] B. Ghanbari, S. Kumar, *A study on fractional predator-prey-pathogen model with Mittag-Leffler kernel-based operators*, Numer. Methods Partial Differential Eq. 40, 2024.
DOI: doi.org/10.1002/num.22689

[42] S. Kumar, R. Kumar, S. Momani, S. Hadid, *A study on fractional COVID-19 disease model by using Hermite wavelets*, Math. Meth. Appl. Sci. 46, 2023.
DOI: 10.1002/mma.7065

[43] S. Kumar, A. Kumar, B. Samet, H. Dutta, *A study on fractional host-parasitoid population dynamical model to describe insect species*, Numer. Methods Partial Differential Eq. 37, 2021.
DOI: 10.1002/num.22603

[44] P. Veeresha, D. G. Prakasha, S. Kumar, *A fractional model for propagation of classical optical solitons by using nonsingular derivative*, Math. Meth. Appl. Sci. 47, 2024.
DOI: 10.1002/mma.6335

[45] Y. Chen, F. Liu, Q. Yu, T. Li, *Review of fractional epidemic models*, Appl. Math. Model. 97, 2021.
DOI: 10.1016/j.apm.2021.03.044

[46] K. Logeswari and C. Ravichandran, *A new exploration on existence of fractional neutral integro-differential equations in the concept of Atangana-Baleanu derivative*, Phys. A 544, 2020.
DOI: 10.1016/j.physa.2019.123454

[47] S. K. Panda, T. Abdeljawad, and C. Ravichandran, *A complex valued approach to the solutions of Riemann-Liouville integral, Atangana-Baleanu integral operator and non-linear telegraph equation via fixed point method*, Chaos Solitons Fractals 130, 2020.
DOI: 10.1016/j.chaos.2019.109439

[48] S. K. Panda, T. Abdeljawad, and C. Ravichandran, *Novel fixed point approach to Atangana-Baleanu fractional and Lp-Fredholm integral equations*, Alex. Eng. J. 59(4), 2020.
DOI: 10.1016/j.aej.2019.12.027

[49] C. Ravichandran, K. Logeswari, and F. Jarad, *New results on existence in the framework of Atangana-Baleanu derivative for fractional integro-differential*

equations, Chaos Solitons Fractals 125, 2019.
DOI: 10.1016/J.CHAOS.2019.05.014

[50] C. Ravichandran K. Logeswari, S. K. Panda, K. S. Nisar, *On new approach of fractional derivative by Mittag-Leffler kernel to neutral integro-differential systems with impulsive conditions*, Chaos Solitons Fractals 139, 2020.
DOI: 10.1016/j.chaos.2020.110012

[51] R. Subashini, K. Jothimani, K. S. Nisar, C. Ravichandran, *New results on nonlocal functional integro-differential equations via Hilfer fractional derivative*, Alex. Eng. J. 59, 2020.
DOI: 10.1016/j.aej.2020.01.055

[52] N. Valliammal, C. Ravichandran, and K. S. Nisar, *Solutions to fractional neutral delay differential nonlocal systems*, Chaos Solitons Fractals 138, 2020.
DOI: 10.1016/j.chaos.2020.109912

[53] J. Losada and J. J. Nieto, *Properties of a new fractional derivative without singular kernel*, Prog. Fract. Differ. Appl. 1, 2015.
DOI: 10.12785/pfda/010202

[54] B. S. T. Alkahtani, A. Atangana, and I. Koca, *Novel analysis of the fractional Zika model using the Adams type predictor-corrector rule for non-singular and non-local fractional operators*, J. Nonlinear Sci. Appl. 10, 2017.
DOI: 10.22436/jnsa.010.06.32

[55] K. Diethelm, *An algorithm for the numerical solution of differential equations of fractional order*, Electron. Trans. Numer. Anal. 5, 1997.

[56] Z. Zhang, *A novel COVID-19 mathematical model with fractional derivatives: Singular and nonsingular kernels*, Chaos Solitons Fractals 139, 2020.
DOI: 10.1016/j.chaos.2020.110060

[57] K. Diethelm, N. J. Ford, and A. D. Freed, *A predictor-corrector approach for the numerical solution of fractional differential equations*, Nonlinear Dynam. 29, 2002.
DOI: 10.1023/A:1016592219341

[58] I. Ahmed, I. A. Baba, A. Yusuf, P. Kumam, W. Kumam, *Analysis of Caputo fractional-order model for COVID-19 with lockdown*, Adv. Differ. Equ., 2020.
DOI: 10.1186/s13662-020-02853-0

[59] R. F. Zhang, M. C. Lin, J. Y. Gan, Q. Li, Z. Z. Lan, *Novel trial function and rogue waves of generalized breaking soliton equation via bilinear neural network method*, Chaos Solitons Fractals, 2022.
DOI: 10.1016/j.chaos.2021.111692